

Article

Comparative Analysis of Helical Piles and Granular Anchor Piles for Foundation Stabilization in Expansive Soil: A 3D Numerical Study

Ammar Alnmr , Richard Paul Ray  and Rashad Alsirawan

Department of Structural and Geotechnical Engineering, Széchenyi István University, 9026 Győr, Hungary; ray@sze.hu (R.P.R.); alsirawan.rashad@sze.hu (R.A.)

* Correspondence: alnmr.ammar@hallgato.sze.hu

Abstract: This study investigates the performance of granular anchor piles and helical piles in expansive soils. Expansive soils pose challenges for engineering due to their significant swelling and shrinkage characteristics. Special considerations are required for constructing foundations on expansive soil to mitigate volumetric changes. While helical piles provide uplift resistance in light structures, they may not fully stabilize foundations in expansive soils. In contrast, granular anchor piles offer a simpler alternative for resisting uplift forces. A numerical study was conducted to analyze the pullout loads, compressive loads, and heave behavior of these anchor techniques. The results demonstrate that granular anchor piles outperform helical piles in terms of pullout and compressive performance, with improvements ranging from 17% to 22.5% in pullout capacity and 0.5% to 19% in compressive capacity, depending on specific pile lengths and diameters examined. However, both techniques show similar effectiveness in reducing heave, achieving reductions of over 90% when specific conditions are met. Additionally, the use of high-rise cap piles contributes to significant heave reduction, effectively minimizing heave to nearly negligible levels compared to low-rise cap piles. It is found that the relative density of the granular material has a more pronounced effect on the pullout load compared to the compressive load, and its impact varies depending on the length of the pile. Therefore, it is recommended to avoid high relative density when the pile is entirely within the expansive soil while utilizing higher relative density is beneficial when the pile penetrates and settles in the stable zone.

Keywords: expansive soils; granular anchor piles; helical piles; pullout load; compressive load; heave behavior; foundation stabilization; numerical simulation



Citation: Alnmr, A.; Ray, R.P.; Alsirawan, R. Comparative Analysis of Helical Piles and Granular Anchor Piles for Foundation Stabilization in Expansive Soil: A 3D Numerical Study. *Sustainability* **2023**, *15*, 11975. <https://doi.org/10.3390/su151511975>

Academic Editors: Xinyu Xie and Kaifu Liu

Received: 24 June 2023
Revised: 25 July 2023
Accepted: 27 July 2023
Published: 3 August 2023



Copyright: © 2023 by the authors. Licensee MDPI, Basel, Switzerland. This article is an open access article distributed under the terms and conditions of the Creative Commons Attribution (CC BY) license (<https://creativecommons.org/licenses/by/4.0/>).

1. Introduction

Expansive soils pose significant challenges to civil engineering structures globally due to their damaging effects [1]. They rank among the six most dangerous natural hazards, including earthquakes, landslides, hurricanes, tornadoes, and floods, according to Baer [2]. Expansive soils and hurricane wind/storm surges are equally ranked in terms of economic losses to buildings. The soil expands and shrinks when moisture content varies, causing significant structural problems in civil engineering structures. During excessive moisture periods, the soil swells, resulting in structure heave, while shrinking occurs during low moisture levels, leading to construction settlement [3]. Additionally, expansive soil applies pressure on vertical foundations, basements, or retaining walls, leading to lateral displacement. Researchers identified that expansive soils undergo volumetric changes in a depth zone ranging from one meter to over 20 m below the ground surface due to seasonal moisture variation [4–7]. This zone is commonly known as the “active” or “unstable” zone [8,9]. Structural damage occurs when volume changes in the active zone of expansive soils occur near foundations. The soil swells excessively when wet and shrinks excessively when dry, creating large surface fissures that may be 20 cm wide and 4 m deep without

warning [10]. Expansive soils present significant challenges to geotechnical engineers worldwide and are found in almost every country [11].

Several researchers explored the possibility of enhancing soil behavior by using special additives [12–17]. Additionally, some investigated the potential of alternative foundation designs, particularly deep foundations, to mitigate the negative effects of the expansive soil [18–23]. The Department of the Army emphasized the significance of foundations in expansive soils and advised opting for cost-effective foundations to reduce structural damage and differential movement between structural elements [24].

Among the various types of deep foundations used in construction sites to support and stabilize structures, helical and granular anchor piles are two notable options. These alternatives are often utilized when conventional foundation techniques, such as deep concrete foundations, are impractical or infeasible [25]. Helical and granular anchor piles were proven effective in both cohesive [26–50] and cohesionless soils [51–56]. These foundations offer economical and environmentally friendly alternatives to conventional methods, and their installation is characterized by speed and efficiency [25].

Moreover, these piles have the potential to facilitate the development of sustainable, cost-effective, and efficient infrastructure, with potential benefits for society. Furthermore, helical and granular anchor piles are capable of providing pullout resistance in various practical applications, including retaining walls, slope and landslide stabilization, and tie-down structures, which are primarily subjected to tensile loads [53,57–59].

Furthermore, helical and granular anchor piles represent feasible alternatives to conventional anchoring techniques. The installation of granular anchor piles is economical and does not require specialized equipment [25,56]. Conducting a comparison between granular anchor piles and established practices, such as helical piles, can provide valuable insights into the positioning of granular anchor piles in the wider spectrum of anchoring methods [56].

Although there are limited studies comparing the performance of granular anchor piles with that of helical piles, Muthukumar and Shukla's research [40] suggests that granular anchor piles are more effective in providing resistance against uplift forces due to their replacement of expansive soil with granular soil, which increases friction at the pile–soil interface. Also, lateral confinement due to swelling enhances the strength of the system. However, this study did not consider the effects of soil disturbance resulting from the installation of helical piles, which would reduce the swelling pressures in the active soil zone and anchor resistance at depth.

Joseph et al. [56] conducted laboratory tests to compare the uplift capacity of granular anchor piles and helical piles. Their results suggest that the former outperformed the latter, but the study was conducted on medium-density sand rather than expansive soil.

Therefore, the objective of this study is to assess and compare the performance of helical and granular anchor piles in expansive soil through numerical simulation using PLAXIS 3D software.

2. Numerical Analysis

In this study, the PLAXIS 3D program was employed to assess the efficacy of helical, and granular anchor piles in mitigating heave induced by expansive soil. The analyses were conducted to determine the pullout and compressive loads of these types of foundations. Given the complexity of the problem and the difficulties associated with laboratory and field tests, numerical analysis emerged as an attractive method for conducting a comparative parametric investigation of the targeted piles in this study [60].

2.1. Plaxis Validation

The primary aim of this section is to verify the precise simulation capabilities of the Plaxis 3D program regarding the behavioral characteristics associated with a heave, the correlation between pullout load and upward movement, and the relationship between compressive load and downward movement for piles in expansive soil. This verification

process serves the overarching objective of obtaining results within a parametric study, facilitating the comparison of reliability and high accuracy among the various parameters under investigation.

Plaxis 3D, a specialized finite element analysis software tailored for geotechnical engineering applications, encompasses a versatile array of elements, degrees of freedom, and critical features crucial to the success of numerical simulations.

The software employs various element types to accurately represent different geotechnical model components. Moreover, 10-node tetrahedral elements are utilized for three-dimensional soil representations, while 3-node line beam elements capture shaft modeling for helical and granular anchor piles. Additionally, 6-node plate elements effectively simulate helices and laboratory model walls, and 12-node interface elements enable a realistic depiction of soil–structure interaction at model boundaries. Interfaces play a crucial role in Plaxis 3D, capturing the interaction between helical or granular anchor piles and surrounding soils. These interfaces facilitate load and deformation transfers, enabling a detailed investigation of pile–soil interface behavior. In the present study, the material model employed for the interfaces aligns with that used for the adjacent soil model. Specifically, R_{inter} (Interface reduction factor) = 0.5 is implemented for the interfaces between the shaft and pile soil, while $R_{\text{inter}} = 1$ is applied for the interfaces between the pile–soil and the surrounding site soil around the pile. Furthermore, gap closure is activated to ensure a more accurate representation of the interface behavior during the numerical simulation.

Plaxis 3D incorporates a comprehensive suite of material models to represent soil and rock behavior. Common models, such as Mohr–Coulomb, Hardening-Soil, Soft-Soil, and Hardening-Soil Small, consider elasticity, plasticity, and hardening aspects, ensuring realistic material responses to applied loads. The hardening soil model chosen for this study is known for its advanced features and reliable results. The Hardening Soil model simulates both soft and stiff soils. In contrast to the Mohr–Coulomb (MC) model, the Hardening Soil (HS) model offers the advantage of considering stress dependency of stiffness, as well as the ability to account for stiffness reduction due to shear strain and a more sophisticated treatment of dilatancy and yield. The HS model provides a wide range of defining parameters, which can be based on laboratory testing or back-calculated from field experience. It demonstrated efficiency in simulating soil behavior, encompassing both soft and stiff soils, and was extensively utilized in various research studies [61–64].

To model soil deformations more accurately in the HS model, a combination of three different stiffness parameters is used at a specific reference stress. These parameters include:

1. Triaxial Loading Stiffness (E_{50}) represents the stiffness of the soil during triaxial loading conditions.
2. Triaxial Unloading–Reloading Stiffness (E_{ur}) represents the stiffness of the soil during the unloading and reloading phases in triaxial tests.
3. Oedometer Loading Modulus (E_{oed}) represents the stiffness of the soil during oedometer loading tests.

The set of parameters entered in the HS model allows the user to distinguish between loading and unloading–reloading stiffnesses. This capability enhances the model’s ability to capture the soil’s response more accurately to various loading conditions and its complex behavior under different stress states [64].

2.1.1. Heave

The verification of Plaxis 3D capability to accurately simulate heave behavior was conducted by calibrating a laboratory experiment detailed in [44], which specifically investigated granular piles in expansive soil, known as black cotton soil. The effectiveness of the granular anchor piles (GAP) system was evaluated through the performance of swell tests on the GAP system. To carry out these tests, a metallic tank with dimensions of 300 mm × 300 mm × 600 mm was employed to establish the soil bed and execute the experimental procedures.

Granular piles with diameters (D) of 30 mm, 40 mm, and 50 mm were installed at a depth (L) of 300 mm. Anchor plates were welded to anchor rods of 8 mm in diameter, with the opposing ends of these rods fastened to a mild steel plate measuring 100 mm \times 100 mm, which served as the surface footing. A layer of sand, 250 mm in thickness (H_1), was uniformly distributed at the bottom of the tank.

A casing pipe with a diameter equal to that of the piles was inserted into the sand bed at the central location within the tank. The anchor plate, attached to the anchor rods, was introduced into the casing pipe, resting on the sand bed. A compacted layer of expansive soil, measuring 300 mm in thickness (H_2), was meticulously placed atop the sand bed, ensuring it corresponded to the maximum dry density and optimum moisture content.

After compacting each layer of expansive soil, the casing pipe was gradually raised to a height below the compacted layer. Then, the pile material was poured into the casing pipe and compacted using a tamping rod, ensuring proper contact between the expansive soil and the pile material. This procedure was repeated until a total height of 300 mm was achieved.

The HS model was employed to simulate the behavior of the soil, with its corresponding parameters outlined in Table 1. Regarding the piles, a linear elastic model was utilized, incorporating Young's modulus of 200 GPa and Poisson's ratio of 0.3.

Table 1. Calibrated soil properties of black cotton soil and sand.

Model Parameter		Black Cotton Soil	Sand
Symbol	Soil Parameters	(Undrained Behavior)	(Undrained Behavior)
γ_{unsat} (kN/m ³)	Unsaturated unit weight	18	16
γ_{sat} (kN/m ³)	Saturated unit weight	21	19
E_{50}^{ref} (kN/m ²)	Reference secant stiffness	3200	40,000
E_{oed}^{ref} (kN/m ²)	Reference tangent stiffness	3200	40,000
E_{ur}^{ref} (kN/m ²)	Reference unloading–reloading stiffness	9600	120,000
C' (kN/m ²)	Cohesion	16	0.01
φ' (°)	Internal friction angle	20	37
Ψ (°)	Dilatancy angle	0	0
ν_{ur} (–)	Unloading/reloading Poisson's ratio	0.2	0.3
m (–)	Exponential power	1	0.5

Figure 1 presents the numerical model and mesh configuration employed for simulating the laboratory models detailed in [44]. To accurately represent the system's geometry and behavior, a coarse mesh was adopted, complemented by local refinement in the vicinity of the pile region. The numerical analysis using PLAXIS 3D closely emulates the laboratory models in terms of dimensions and incorporates three phases to simulate the laboratory installation process:

- In the first phase, a borehole was created to facilitate the installation of the granular anchor pile. This entailed deactivating the corresponding soil volume and subsequently activating the anchor plate, anchor rod, and granular anchor material.
- The second phase involved the activation of the footing plate on the expansive soil within the model.
- Finally, in the third phase, a suitable volumetric strain was applied to the expansive soil volume to accurately simulate heave behavior.

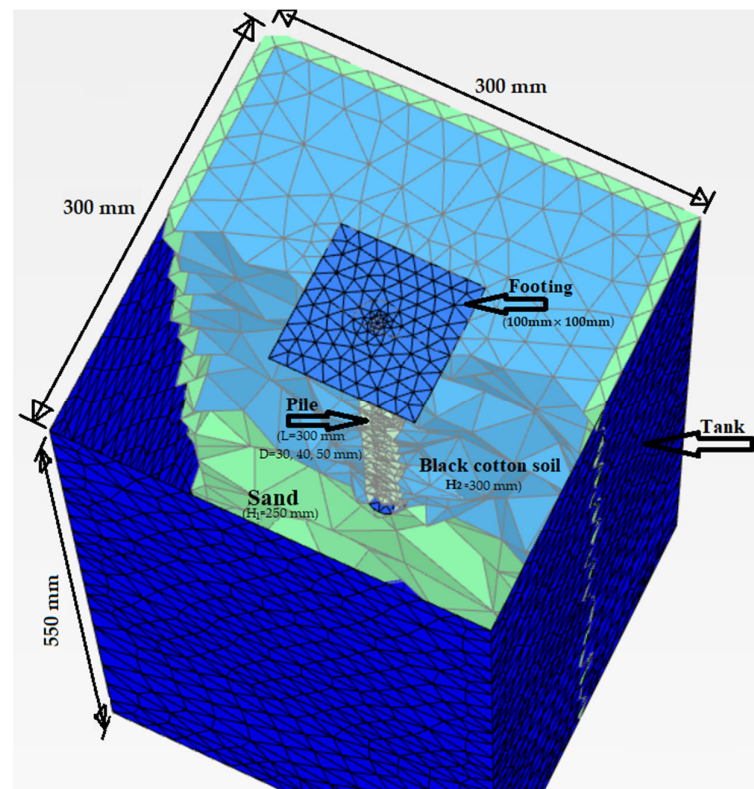


Figure 1. Numerical model and mesh configuration employed for simulating the laboratory models detailed in [44].

Figure 2 showcases a comparative analysis between the heave results obtained from Plaxis 3D program and the experimental findings for the three different pile diameters. A volumetric strain of 2% was applied during the simulations. It is worth noting that certain disparities were observed between the simulation results and the experimental data. These disparities can be attributed to the uniform saturation conditions applied in the laboratory experiments, which cannot be precisely replicated through the volumetric strain approach in numerical simulations.

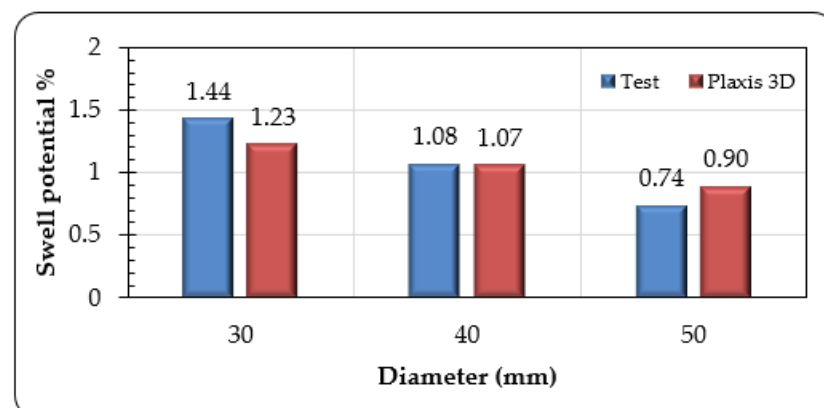


Figure 2. Comparison of heave results between plaxis program and experimental results for the three different diameters.

Nevertheless, the overall performance of the simulations yielded acceptable results. The volumetric strain method proves to be an effective approach for simulating heave behavior, particularly when the direction of saturation is explicitly defined, either from

the top or bottom. Consequently, this methodology will be adopted in the forthcoming parametric study to investigate and analyze various studied parameters.

The behavior of heave was also simulated for the experimental test conducted in accordance with [65]. The experimental setup involved a cylindrical aluminum tank with an internal diameter of 300 mm and a height of 700 mm. The model pile, made of aluminum, had an outer diameter (D_a) of 25.4 mm, a wall thickness (t) of 3 mm, and a height (L) of 600 mm.

In the initial step, the prefabricated model pile was securely fixed to the loading machine, using a bolt to maintain its fixed position during the compaction process. A waterproof ruler was affixed to the inner wall of the aluminum tank. Next, fine sand was poured into the tank to a height (H_1) of 150 mm, and a floating model pile was placed on the sand layer. Following these preparations, the expansive soil, pre-mixed with a water content of 27%, was compacted to achieve a wet density of 17.36 kN/m^3 . The buried length of the model pile within the expansive soil was 400 mm.

In the subsequent step, a service load of 500 N was applied to the pile head prior to water infiltration. After attaining a stable pile displacement, water was added to the top surface. These steps were replicated using the Plaxis 3D program. The HS model was employed to simulate the behavior of the soil, with its parameters specified in Table 2. A volumetric strain of 7.6% was applied. For the piles, a linear elastic model was used, with Young's modulus of 69 GPa and Poisson's ratio of 0.3.

Table 2. Calibrated soil properties of Regina clay and sand.

Model Parameter		Regina Clay (Undrained Behavior)	Sand (Drained Behavior)
Symbol	Soil Parameters		
γ_{unsat} (kN/m^3)	Unsaturated unit weight	17.36	17
γ_{sat} (kN/m^3)	Saturated unit weight	18.4	19
E_{50}^{ref} (kN/m^2)	Reference secant stiffness	12,500	1300
E_{oed}^{ref} (kN/m^2)	Reference tangent stiffness	14,000	1300
E_{ur}^{ref} (kN/m^2)	Reference unloading–reloading stiffness	37,500	3900
C' (kN/m^2)	Cohesion	17	10
φ' ($^\circ$)	Internal friction angle	15.6	38
Ψ ($^\circ$)	Dilatancy angle	4	8
ν_{ur} (–)	Unloading/reloading Poisson's ratio	0.25	0.2
m (–)	Exponential power	0.95	0.5

Figure 3 illustrates the numerical model and mesh configuration, employing a coarse mesh with localized refinement around the pile region. The numerical analysis, conducted using PLAXIS 3D, effectively replicates the laboratory models in terms of dimensions and incorporates three phases to simulate the laboratory installation process:

- In the first phase, a borehole was created to facilitate the installation of the prefabricated model pile. This entailed deactivating the corresponding soil volume and subsequently activating the prefabricated model pile.
- In the second phase, the load of 500 N applied to the pile head was activated.
- Finally, in the third phase, a suitable volumetric strain (7.6%) was applied to the expansive soil volume from top to bottom to accurately simulate heave phenomena as it was in the laboratory.

Figure 4 illustrates the comparison of final heave results obtained for both the pile and the surrounding soil, indicating good agreement. This confirms the capability of Plaxis 3D, using the volumetric strain approach, to accurately simulate uplift behavior in expansive soil.

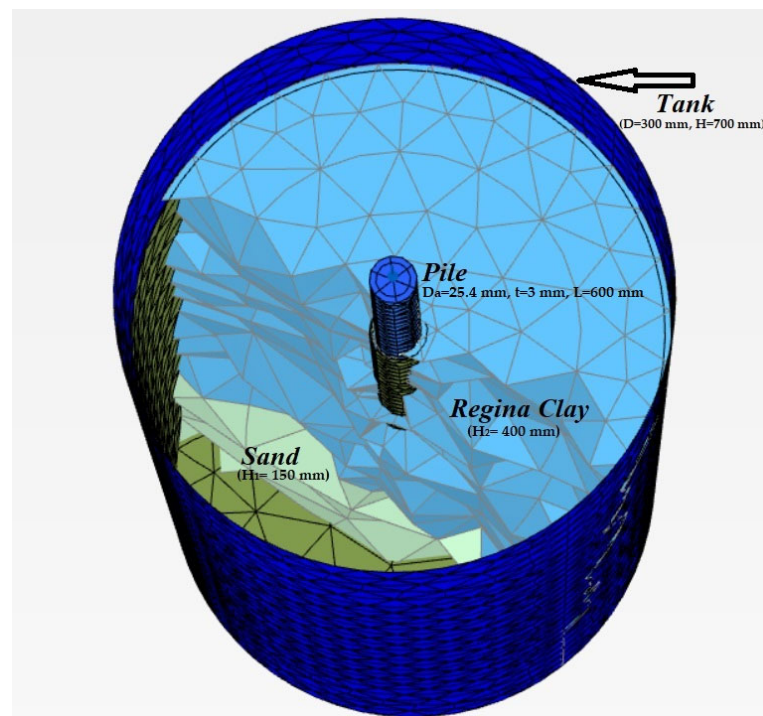


Figure 3. Numerical Model and Mesh Used for Simulating the Laboratory Model Detailed in [65].

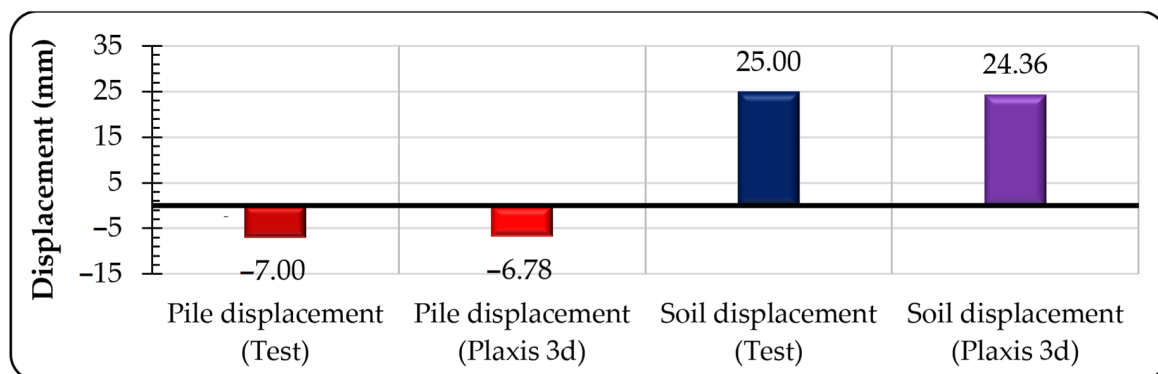


Figure 4. Comparison of final displacements in both pile and surrounding soil.

2.1.2. Pullout

The capability of Plaxis 3D to simulate pullout behavior was verified by calibrating the same laboratory experiment described in [44], which focused on granular anchor piles (GAPs) in expansive soil. Modifications were made to the previous setup to determine the pullout capacity of the granular anchor pile foundation (GAPF) system. A pulley was fixed to the horizontal bar at the top of the tank, and the surface footing was not provided. The top end of the anchor rod was attached to a hook connected to a string passing over the pulley. The opposite end of the string was fixed to a loading hanger. A dial gauge was installed to measure the vertical displacement of the GAP.

The load, applied in 10% increments of the expected value, was gradually increased on the hanger, and the corresponding readings from the dial gauge were recorded. The loading process continued until failure occurred.

Figure 5 illustrates the comparison between the load–displacement curves obtained using the Plaxis 3D program and the experimental results. The results show good agreement, confirming the capability of the Plaxis 3D program to simulate the pullout behavior of piles in expansive soil.

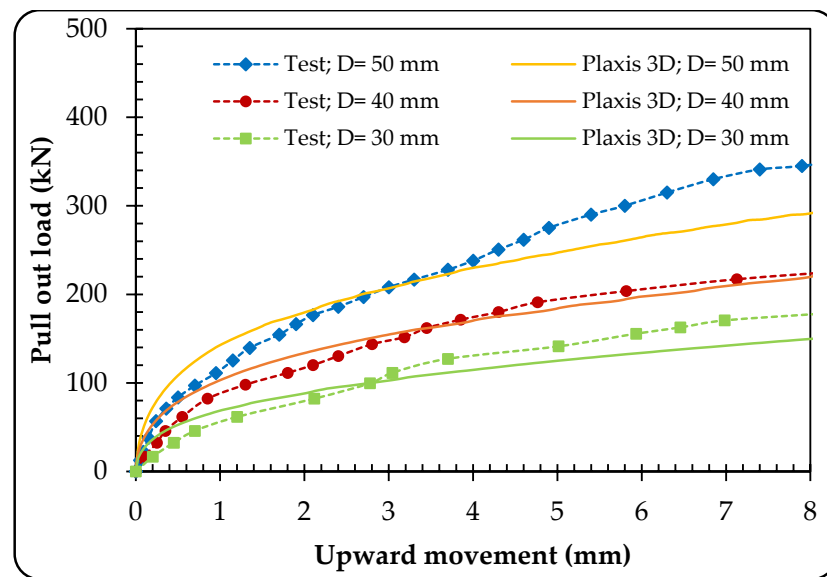


Figure 5. Comparison of pullout load–upward movement curves obtained using the Plaxis Program and experimental results for the three different diameters.

2.1.3. Compressive Behavior

The capacity of the Plaxis 3D software to accurately simulate the compressive behavior of helical piles in clayey soil (Site B) was assessed in this study. The verification process involved referencing the experiments conducted in previous studies [66,67].

To replicate the soil behavior, the HS model was employed, utilizing the parameters specified in Table 3. The helical piles were modeled using a linear elastic approach, with Young's modulus of 200 GPa and Poisson's ratio of 0.3.

Table 3. Calibrated soil properties at site B.

Model Parameter		Layer 1 Depth 0–3.5 m		Layer 2 Depth 3.5–9 m	Layer 2 Depth 3.5–6.8 m
		Undisturbed (Undrained Behavior)	Disturbed (Undrained Behavior)	Undisturbed (Undrained Behavior)	Disturbed (Undrained Behavior)
Symbol	Soil Parameters				
γ_{sat} (kN/m ³)	Saturated unit weight	17.5	17.5	15.5	15.5
E_{50}^{ref} (kN/m ²)	Reference secant stiffness	21,000	15,000	10,000	8000
$E_{\text{oad}}^{\text{ref}}$ (kN/m ²)	Reference tangent stiffness	24,650	18,500	16,350	15,100
$E_{\text{ur}}^{\text{ref}}$ (kN/m ²)	Reference unloading–reloading stiffness	63,000	45,000	30,000	24,000
C' (kN/m ²)	Cohesion	8	6	1.8	1.4
φ' (°)	Internal friction angle	20	15	10.5	8.2
Ψ (°)	Dilatancy angle	0	0	0	0
ν_{ur} (–)	Unloading/reloading Poisson's ratio	0.2	0.2	0.2	0.2
m (–)	Exponential power	1	1	1	1

The helical pile used in the investigation had a length (L) of 7.2 m and consisted of three helices with a diameter (D_p) of 0.61 m and a thickness of 20 mm. The spacing between the helices (S/D_p) was set at 3. The shaft diameter (D_s) was 0.178 m, with a wall thickness (t) of 8.1 mm.

Figure 6 illustrates the numerical model and mesh configuration, which utilized a coarse mesh with localized refinement around the pile region. The numerical analysis, conducted using PLAXIS 3D, effectively replicated the field test, considering the dimensions of the pile and an adequate model size to mitigate boundary effects on the results. The model width to the pile diameter ratio was designed to be greater than 12 [68]. The simulation followed a two-phase approach to simulate the field installation process:

- In the first phase, the helical pile was activated, involving deactivating the corresponding soil, followed by activating anchor plates, anchor rods, and disturbed soils of layer 1 and layer 2.
- In the second phase, a downward prescribed displacement of 40 mm on the pile head was activated.

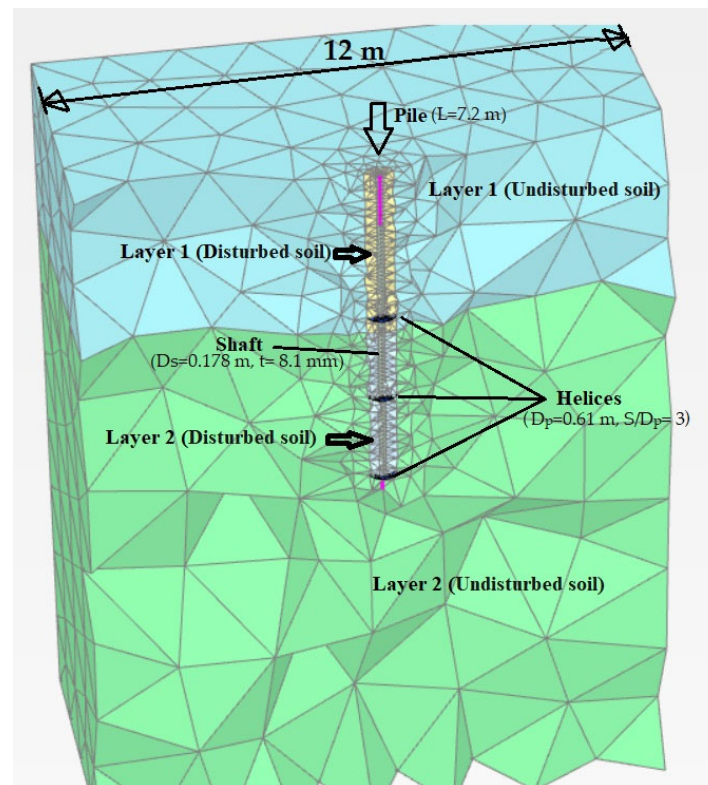


Figure 6. Numerical model and mesh configuration.

Figure 7 presents a comparative evaluation of the results obtained from the Plaxis program and the field test data. The comparison demonstrates the commendable ability of the Plaxis software to effectively simulate the compressive behavior of helical piles in clayey soil, as validated by the agreement between the numerical and experimental outcomes.

2.2. Problem Description

The present study aims to investigate the performance of a shallow square footing resting on an expansive soil layer and reinforced with either a single granular anchor pile or a helical pile. To accomplish this objective, varying lengths and diameters of piles are used as input parameters for analysis, as listed in Table 4. Moreover, the cap widths are also altered, with widths of 1, 2, and 4 m being studied at fixed pile lengths and diameters of 7 m and 0.6 m, respectively. The effect of raised caps is also examined. Additionally, the influence of the relative density of the granular material used in the granular anchor piles is considered. The active zone of the expansive soil layer extends from the surface to a depth of 4 m, where stable, saturated, dense sand is present beneath with a thickness of 10 m.

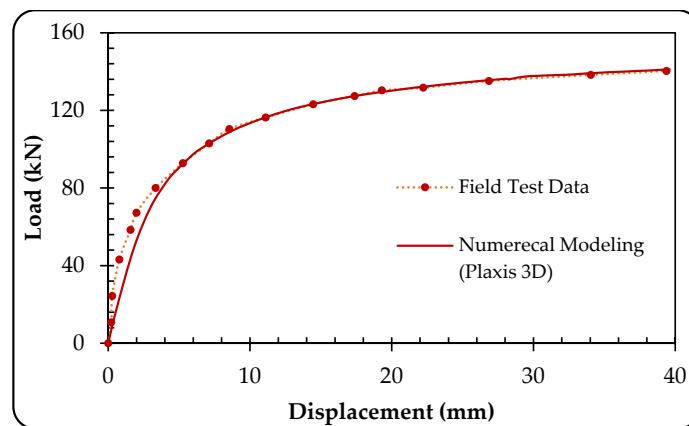


Figure 7. Load–displacement curves of calibrated numerical model using Plaxis 3D and field-tested pile in clayey soil.

Table 4. Problem dimensions in this study.

Granular Anchor Pile Length (L) (m)	Diameter (D) (m)	Cap Width (B) (m)
4	0.3, 0.6, 0.9	1
7	0.3, 0.6, 0.9	1, 2, 4
10	0.3, 0.6, 0.9	1

2.3. Methodology

The present study employs the same methodology and materials properties as Alnmr et al. [69]. For further details, please refer to [69]. Figure 8 illustrates a cross-sectional view of unreinforced and reinforced soil with helical and granular anchor piles. The ratio of the model width to the pile diameter of the model pile was designed to be around 12, which is considered satisfactory to alleviate the influence of boundary effects on the results of unsaturated soils [68]. The 3D model is employed to calculate heave for various parameters of granular anchor piles and helical piles mentioned in Section 2.2. Saturation conditions are modeled by considering water infiltration from the top and rising groundwater from the bottom. Numerical analysis comparisons are facilitated by evaluating the pullout load and the compressive load.

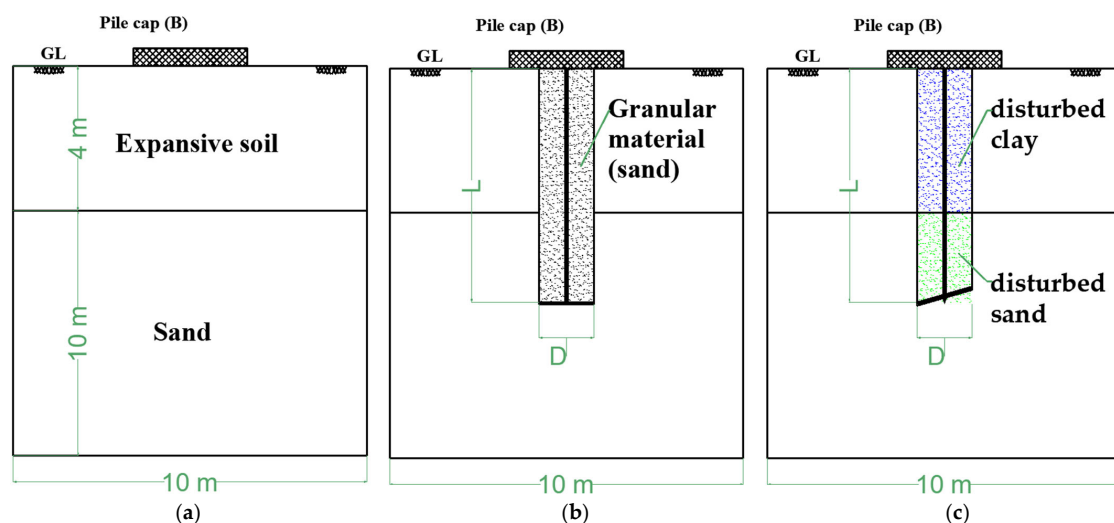


Figure 8. Cross-sectional view of (a) unreinforced soil, (b) granular anchor pile, and (c) helical pile [69].

Boundary and Initial Conditions

The lateral boundaries of the model are assumed to have zero horizontal displacements, and the bottom has zero horizontal and vertical displacements. This assumption reflects the natural behavior of the soil, where the surrounding soil at a large horizontal distance acts as horizontal fixities [70]. Once all inputs were assigned, the program Plaxis 3D generated a mesh, as illustrated in Figure 9. A coarse mesh was utilized for both types of piles, but some refinement was implemented around the piles. The total number of soil elements used in the analysis was 14,526, and the number of nodes was 22,207. Figure 9 presents a detailed illustration of the expansive soil layer, sand layer, pile, footing, and the employed mesh. The numerical simulation incorporates seven distinct phases, each playing a crucial role in comprehensively analyzing the behavior of the system:

- Phase 1: In this phase, a borehole is created to facilitate the installation of either the helical or granular anchor pile. The process involves deactivating the respective soil volume, followed by the activation of the anchor plate, anchor rod, and granular anchor material or disturbed sand and clay, as required.
- Phase 2: The footing plate is activated.
- Phase 3: The third phase entails applying a load of 40 kN to the footing.
- Phase 4: In the fourth phase, a suitable volumetric strain is applied to the expansive soil volume in the model input window, specifically from top to bottom, as demonstrated in Figure 15.
- Phase 5: The fifth phase commences after the third phase, where the same volumetric strain of 8% is applied in the reverse direction, i.e., from bottom to top, as depicted in Figure 15.
- Phase 6: Following the second phase, the sixth phase involves activating an upward prescribed displacement of 25 mm on the surface footing is activated to calculate the upward load.
- Phase 7: Lastly, in the seventh phase, which also commences after the second phase, a downward prescribed displacement of 25 mm on the surface footing is activated to calculate the downward load.

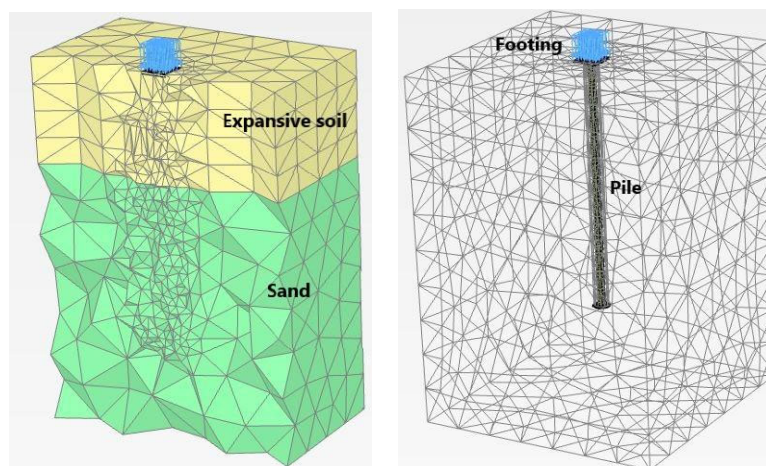


Figure 9. Mesh configuration of the analyzed model [69].

In this study, the water table was assumed to be at the base of the expansive soil during the initial condition assignment. Then, the initial stresses were calculated using Jacky's formula with coefficients of earth pressure at rest, $K_0 = 0.536$ and $K_0 = 0.4$ for expansive soil and sand, respectively, where $K_0 = 1 - \sin \varphi$. The change in volumetric strain was utilized to simulate the heave of the clay in the analysis, which exhibited a positive volumetric strain and was related to the degree of saturation in the expansive soil. Tripathy et al. [71] determined that complete swelling occurs at a water content of 30%, following an S-shaped curve. For highly plastic clays with porosities ranging from 0.4 to

0.6, the degree of saturation equivalent to 30% moisture content would be approximately 90% [72]. Therefore, the moisture-swell function was used to provide 100% swelling at a saturation level of around 90% (Figure 10). Al-Shamrani and Dhowian [73] demonstrated that data from the triaxial compression test predicted field measurements of surface heave, and they found that the results of the traditional oedometer test were about 1/3 as accurate as the actual surface heave. Accordingly, this study utilized an 8% positive volumetric strain for comparison, which is equivalent to 1/3 of the maximum free swell value obtained by Thakur and Singh [74].

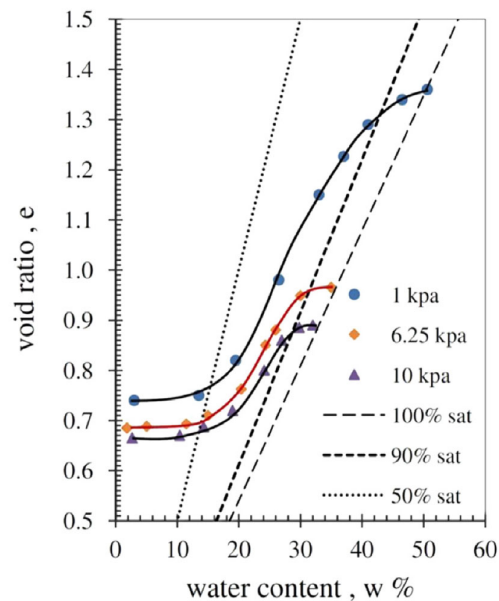


Figure 10. S-shaped curves illustrating the effect of various surcharges on expansive soil [72].

3. Results and Discussion

3.1. Effect of Pile Length (L) and Diameter (D)

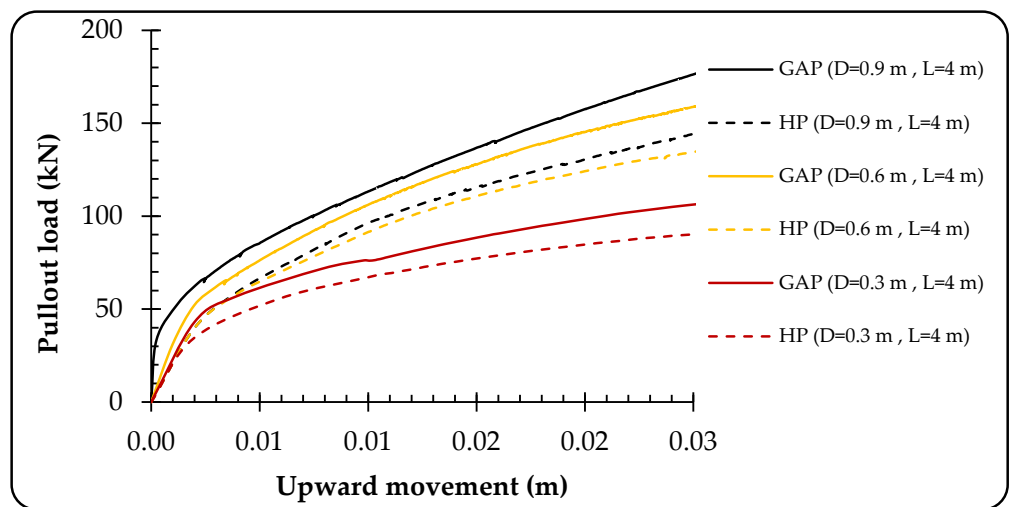
The influence of variations in length and diameter of helical and granular anchor piles on their pullout load behavior and compressive load behavior was investigated to enable an effective comparison between them. Three different lengths were considered, and for each length, three different diameters were taken into account, as outlined in Table 4.

For a length of 4 m, it corresponds to the occurrence of the pile within the expansive soil layer exclusively. In the case of the remaining two lengths, 7 and 10 m, it was assumed that the piles were embedded in a strong soil layer (sandy soil) at depths of 3 and 6 m, respectively.

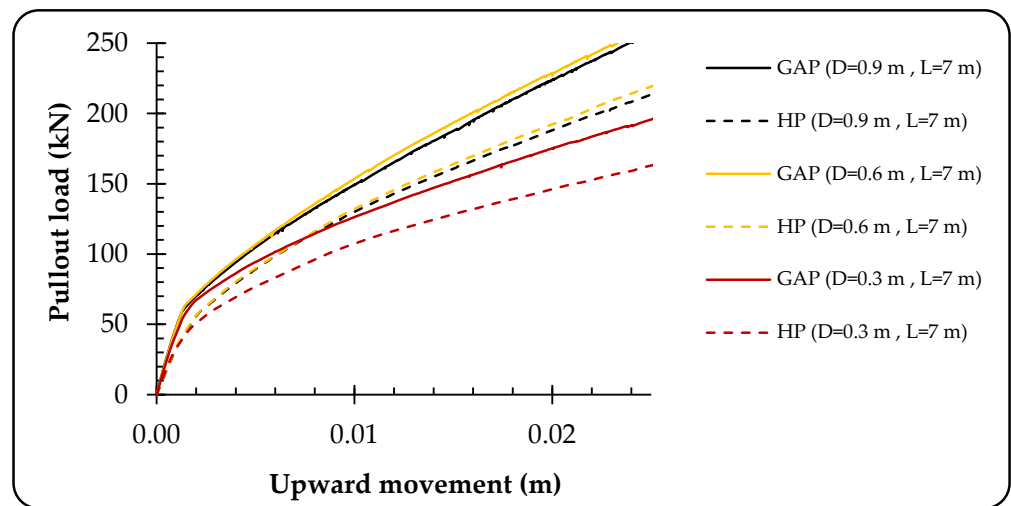
3.1.1. Impact of Pile Length (L) and Diameter (D) on Pullout Behavior

Figure 11 illustrates the load–displacement curves representing the pullout behavior of different lengths and diameters of granular anchor piles and helical piles. These curves provide a visual understanding of how the piles respond to upward movement, and they highlight the variations in pullout loads associated with different pile lengths and diameters.

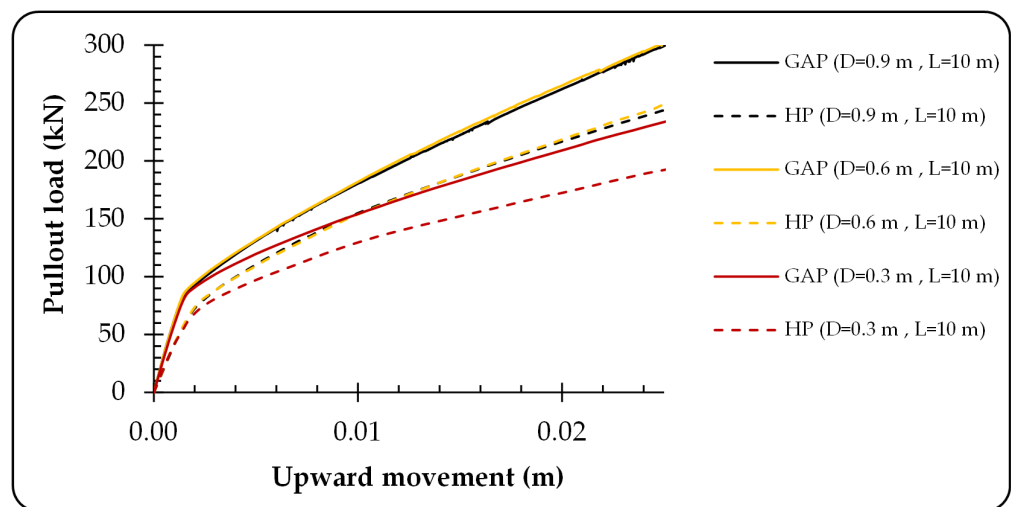
The investigation aimed to examine the effect of varying the length and the diameter of granular anchor piles and helical piles on the pullout load required to resist an upward movement of 25 mm. The results, presented in Table 5, reveal that increasing the length of both the granular anchor pile and the helical pile results in an increase in the pullout load. This suggests that longer piles are more effective in resisting upward movement.



(a)



(b)



(c)

Figure 11. Pullout behavior of granular anchor piles and helical piles at different diameters: (a) L = 4 m, (b) L = 7 m, (c) L = 10 m.

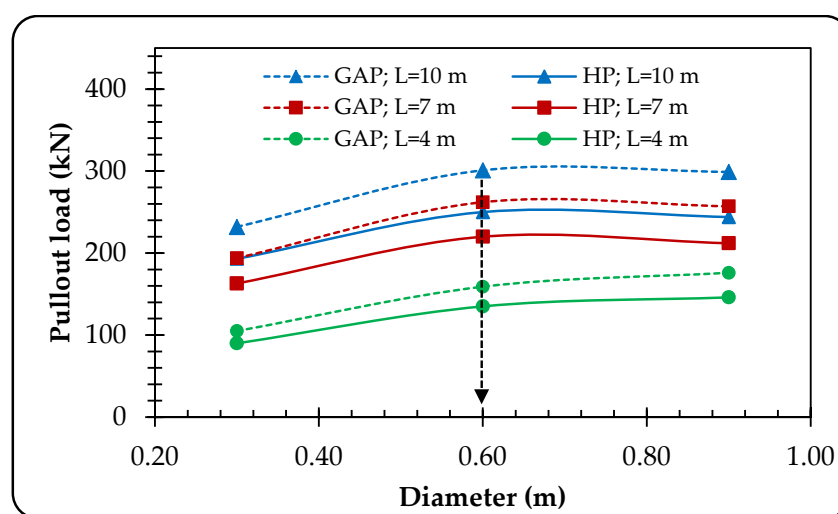
Table 5. Comparison of pullout loads between helical piles (HP) and granular anchor piles (GAP).

D (m)	L (m)	GAP Pullout Load (kN)			HP Pullout Load (kN)			(GAP – HP)/HP (%)		
		4	7	10	4	7	10	4	7	10
0.30		105	194	232	90	163	193	16.7	19.0	20.2
0.60		159	262	301	135	220	250	17.8	19.1	20.4
0.90		176	257	299	146	212	244	20.5	21.2	22.5

Significantly, the performance of the granular anchor pile surpasses that of the helical pile, as evidenced by the data in Table 5. The granular anchor pile demonstrates an improvement in pullout load ranging from 17% to 22.5% compared to the helical pile. This difference can be attributed to the larger contact area between the granular anchor pile and the surrounding soil. The increased contact area enhances the friction resistance, enabling the granular anchor pile to withstand higher loads.

In contrast, the installation of the helical pile introduces disturbances to the soil and weakens its overall strength. Consequently, the helical pile experiences reduced resistance, leading to lower pullout loads compared to the granular anchor pile.

Moreover, the impact of pile diameters on the pullout load, specifically in relation to a 25 mm upward movement, is depicted in Figure 12 for various lengths of helical and granular anchor piles. Notably, a trend is observed where the pullout load experiences a slight increase, stabilizes, or slightly decreases after a diameter of 0.6 m. This behavior can be elucidated by considering multiple contributing factors.

**Figure 12.** Relationship between pullout load and diameter.

The interaction between the pile and the surrounding soil is an intricate phenomenon that is influenced by diverse factors, encompassing soil type, soil properties, and installation methods. This interaction signifies the interdependence of the pile and soil behavior, implying that alterations in one element can impact the other. Upon surpassing a specific diameter, the interaction between the pile and the soil may reach a state of equilibrium, resulting in a stabilized or slightly diminished pullout load.

In addition, enlarging the pile diameter engenders a greater contact area between the pile and the surrounding soil. This augmented contact area significantly enhances the frictional resistance, which plays a pivotal role in counteracting the upward forces exerted during pullout. However, there exists a threshold beyond which further increases in the pile diameter yield diminishing returns in terms of contact area expansion. In the context of this study, this threshold is identified as 0.6 m. Beyond this diameter, the additional gains

in contact area become relatively less substantial, consequently leading to a stabilization or slight reduction in the pullout load.

Based on these findings, it is recommended that a minimum pile diameter of 0.6 m be employed to ensure an adequate load-bearing capacity and stability of the piles. This diameter threshold ensures an optimized balance between contact area expansion, frictional resistance, and pullout load, thereby enhancing the overall performance and reliability of the pile foundation system.

3.1.2. Impact of Pile Length (L) and Diameter (D) on Compressive Load

This investigation aimed to assess the influence of varying the lengths and diameters of granular anchor piles (GAP) and helical piles (HP) on their ability to withstand compressive loads and resist downward movement. A comprehensive overview of the recorded loads for both pile types is presented in Table 6, while Figure 13 provides a visual representation of the compressive load behavior for different pile lengths, offering valuable insights into their response under compressive loading conditions and highlighting the variations in load resistance associated with varying pile lengths.

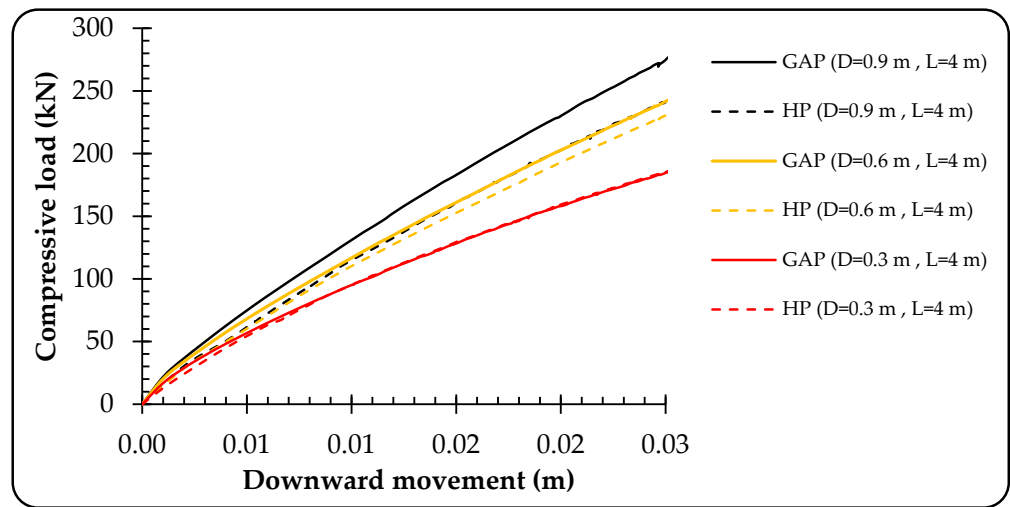
Table 6. Comparison of compressive load resistance between granular anchor piles (GAP) and helical piles (HP).

		GAP Pullout Load (kN)			HP Pullout Load (kN)			(GAP – HP)/HP (%)		
D (m)	L (m)	4	7	10	4	7	10	4	7	10
	0.30		186	226	263	185	216	249	0.5	4.6
0.60		241	280	319	230	255	286	4.8	9.8	11.5
0.90		275	301	342	242	253	287	13.6	19.0	19.2

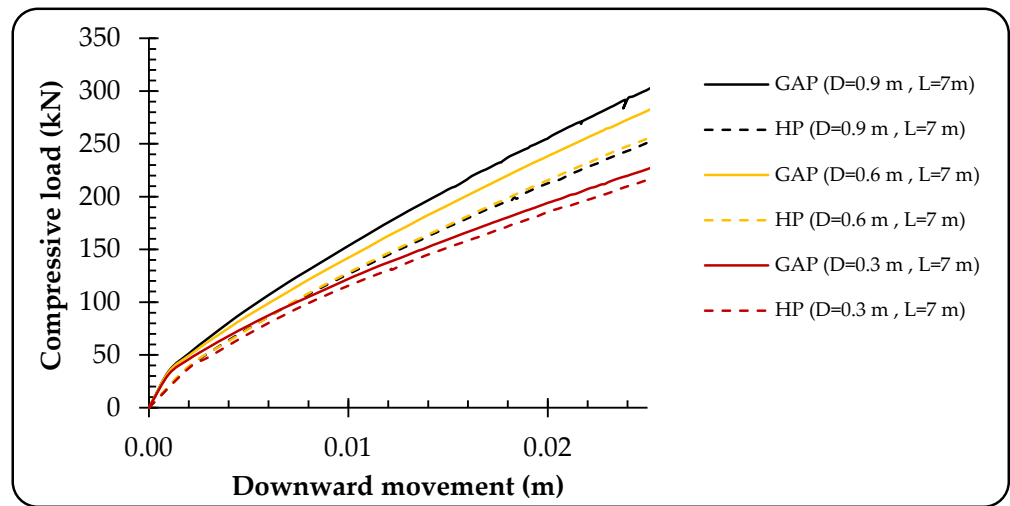
The findings from Table 6 reveal that increasing the length of both GAP and HP enhances their load resistance capabilities, indicating that longer piles are more effective in withstanding compressive loads and resisting downward movement. This observation suggests that the additional length provides increased bearing capacity and improves the overall stability of the piles.

Furthermore, the impact of pile diameters on the compressive load, specifically in relation to a 25 mm downward movement, is depicted in Figure 14 for various lengths of helical and granular anchor piles. Notably, a significant trend is observed where the compressive load continues to increase for the GAP piles. However, for the HP piles, a stabilization or a slight increase is observed after a diameter of 0.6 m. This behavior can be attributed to the interaction between the piles and the surrounding soil.

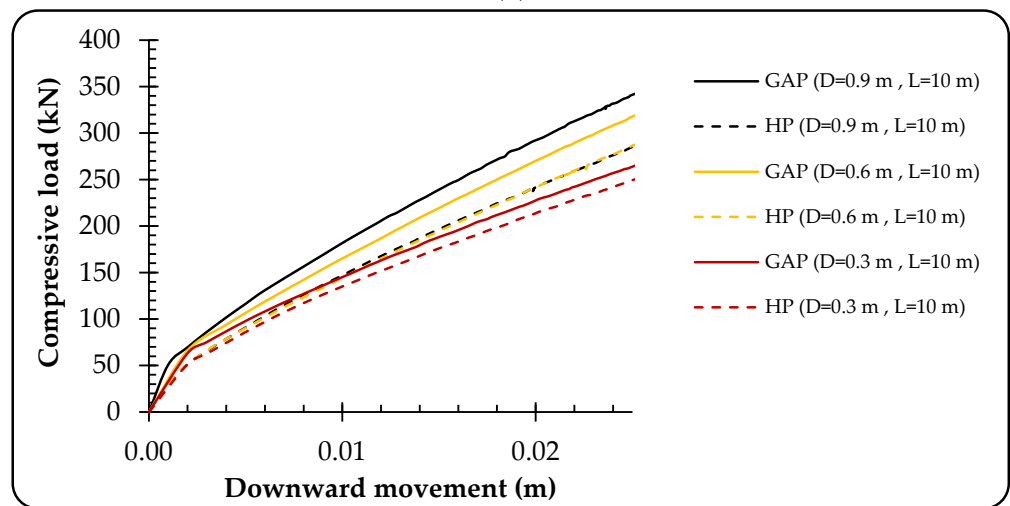
The superior load resistance exhibited by the granular anchor pile, as indicated by the data in Table 6, highlights its advantage over the helical pile. The granular anchor pile demonstrates a 0.5% to 19% improvement in performance compared to the helical pile. This performance discrepancy can be attributed to the inherent characteristics of the granular anchor piles, which provide a larger contact area with the surrounding soil. The presence of granular materials allows for enhanced frictional resistance, resulting in an increased load-bearing capacity. The larger contact area facilitates a more efficient transfer of loads from the piles to the soil, enabling the granular anchor piles to withstand higher compressive loads and provide improved stability.



(a)



(b)



(c)

Figure 13. Compressive load response of granular anchor piles and helical piles at various diameters; (a) Pile Length (L) = 4 m, (b) Pile Length (L) = 7 m, (c) Pile Length (L) = 10 m.

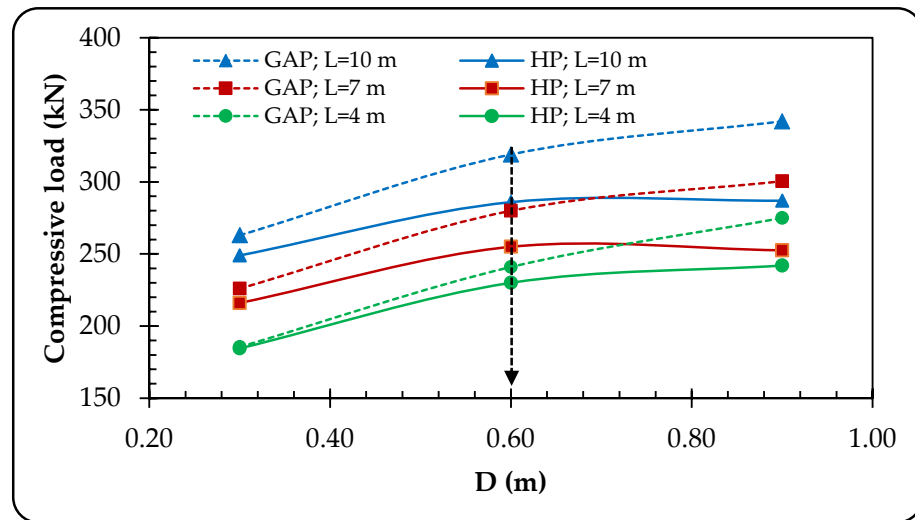


Figure 14. Influence of pile diameter on compressive load.

3.1.3. Impact of Pile Length (L) and Diameter (D) on Heave

In this section, the influence of pile length and diameter on heave reduction is investigated for three different lengths and diameters of granular anchor piles and helical piles. The analysis focuses on understanding the effects of moisture saturation, considering two scenarios: (1) downward saturation from the top (rainfall infiltration) and (2) upward saturation from the bottom (groundwater rise). The heave comparison involves examining the movement as each successive meter of the active zone undergoes saturation until reaching complete saturation. To provide visual clarity, Figure 15 depicts the potential directions of moisture migration during the heaving process.

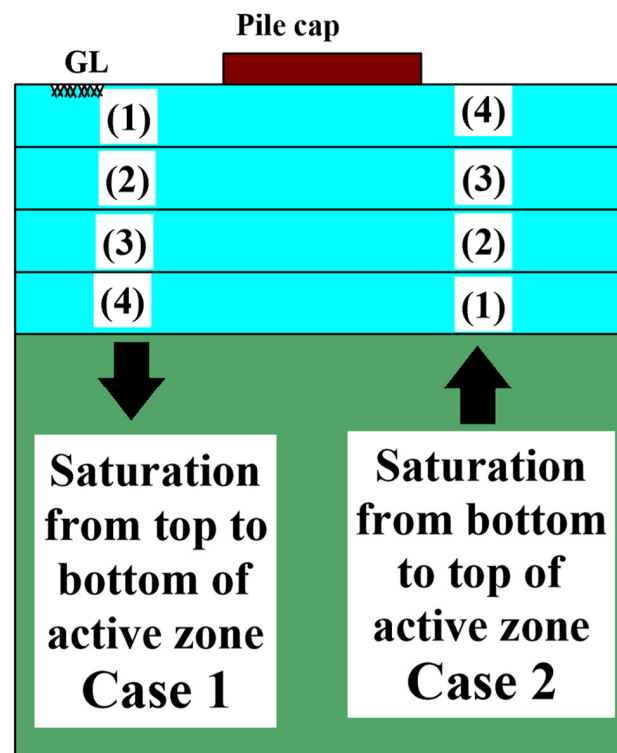


Figure 15. Numbering of active zone parts for two cases of saturation: sequential saturation of partial layers in expansive soil (numbering: 1, 2, 3, and 4) [69].

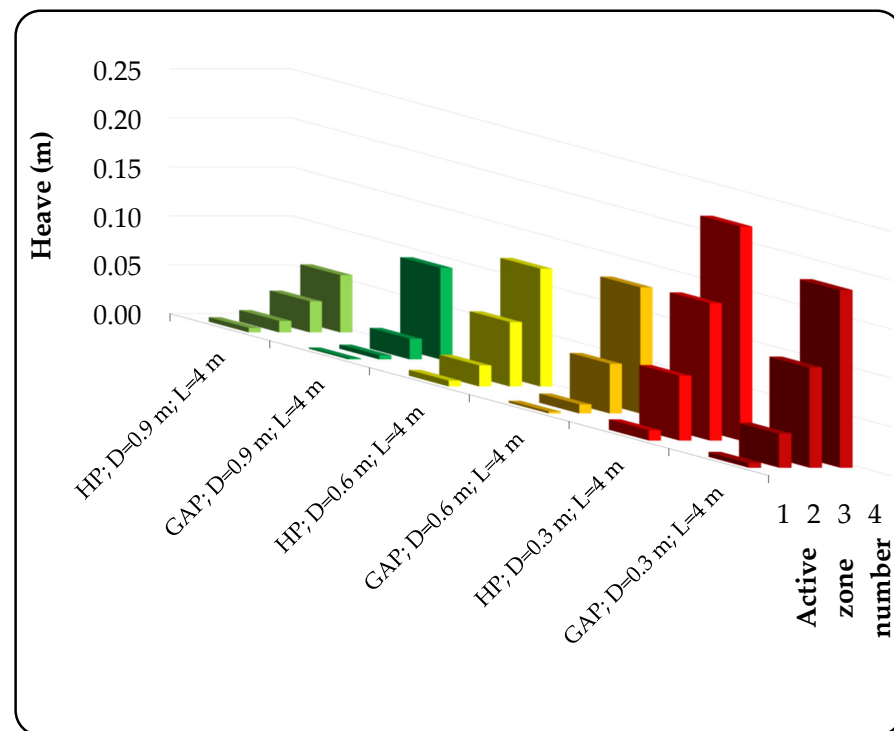
Starting Saturation from the Top (Case 1)

An investigation was conducted to examine the influence of the pile diameter and the length on the performance of helical and granular piles regarding their heave behavior under the condition of top-down saturation. The obtained results provide valuable insights into the unique heave behavior demonstrated by these piles.

The numerical findings, as illustrated in Figure 16, reveal that an increase in pile diameter enhances the performance of helical piles compared to granular piles. This can be attributed to the installation process of helical piles, which leads to the disturbance and degradation of the expansive soil. Consequently, the swelling capacity of the soil is reduced. In contrast, granular piles experience an increase in lateral surface area as the diameter increases, resulting in improved interaction with the expansive soil and, consequently, higher forces acting on the piles when they become saturated.

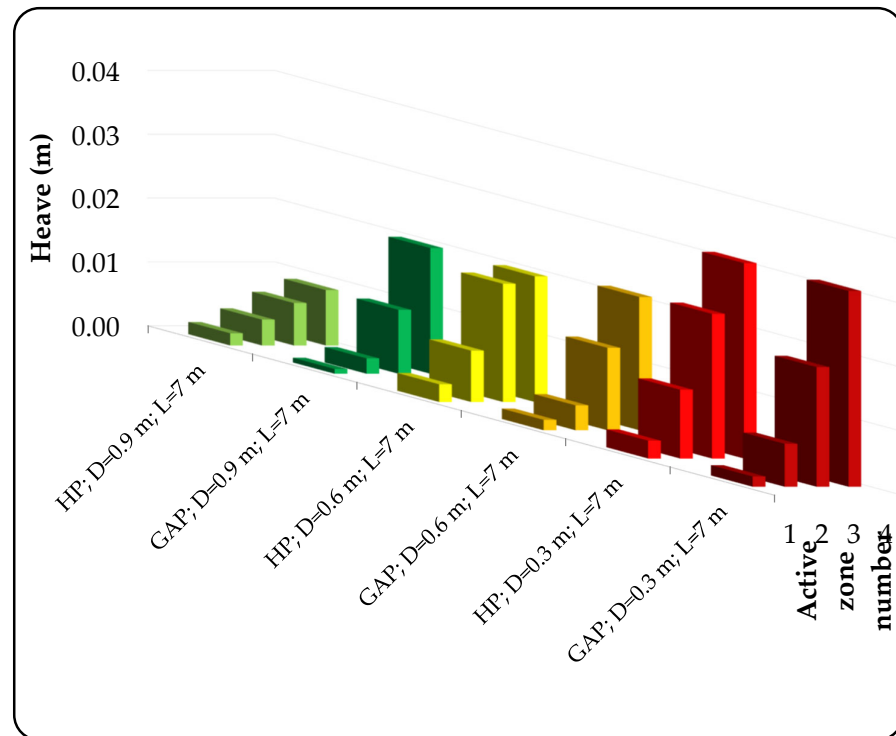
Another significant observation is that the penetration of both types of piles into the stable zone causes a substantial reduction in pile heave. The confinement stress exerted by the surrounding soil increases, reinforcing the resistance to soil expansion. Moreover, as the confinement stress increases with the depth, the helical piles exhibit a more secure anchorage compared to granular piles. It should be noted that these findings align with a previous study conducted by Muthukumar and Shukla [40], with slight discrepancies attributed to the smaller scale of their experiments.

Table 7 presents the reduction in heave achieved by both helical and granular piles in comparison to the case of unreinforced soil. When the pile penetrates the stable layer, the heave reduction values are relatively close for both pile types. However, in cases where the entire pile is located within the active zone ($L = 4$ m) and has a small diameter ($D = 0.3$ m), the performance of granular piles surpasses that of helical piles. Nevertheless, as the pile diameter increases, the helical piles regain their superiority over granular piles, as explained above.

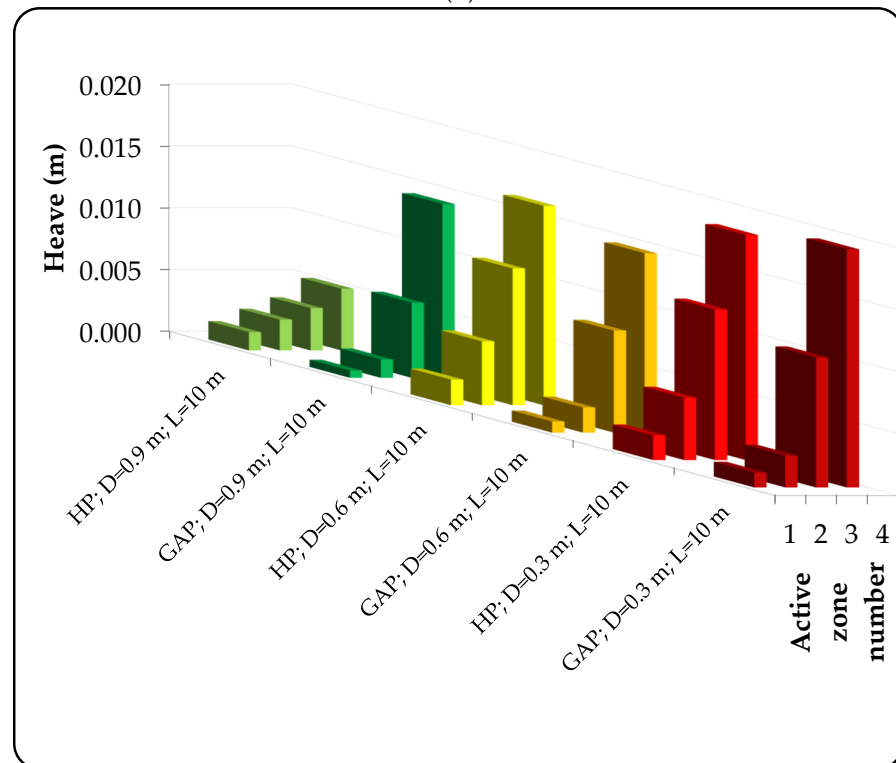


(a)

Figure 16. Cont.



(b)



(c)

Figure 16. Heave at different diameters of helical and granular anchor piles for Case 1. (a) L = 4 m, (b) L = 7 m, (c) L = 10 m.

Table 7. Uplift reduction of both helical piles and granular anchor piles compared to unreinforced soil in Case 1.

D (m)	L (m)	Heave Reduction of Granular Anchor Pile (%)			Heave Reduction of Helical Pile (%)		
		4	7	10	4	7	10
0.3		32.20	88.55	92.82	18.25	88.57	93.21
0.6		51.79	92.21	93.04	55.00	92.65	93.99
0.9		65.04	92.65	94.76	78.12	96.76	98.14

The relationship between heave reduction and the ratio of pile length (L) to the thickness of the active zone (H) is depicted in Figure 17. The results clearly demonstrate that increasing the pile length significantly reduces heave. To achieve a substantial 90% reduction in uplift, it is recommended to have an L/H ratio greater than 1.8.

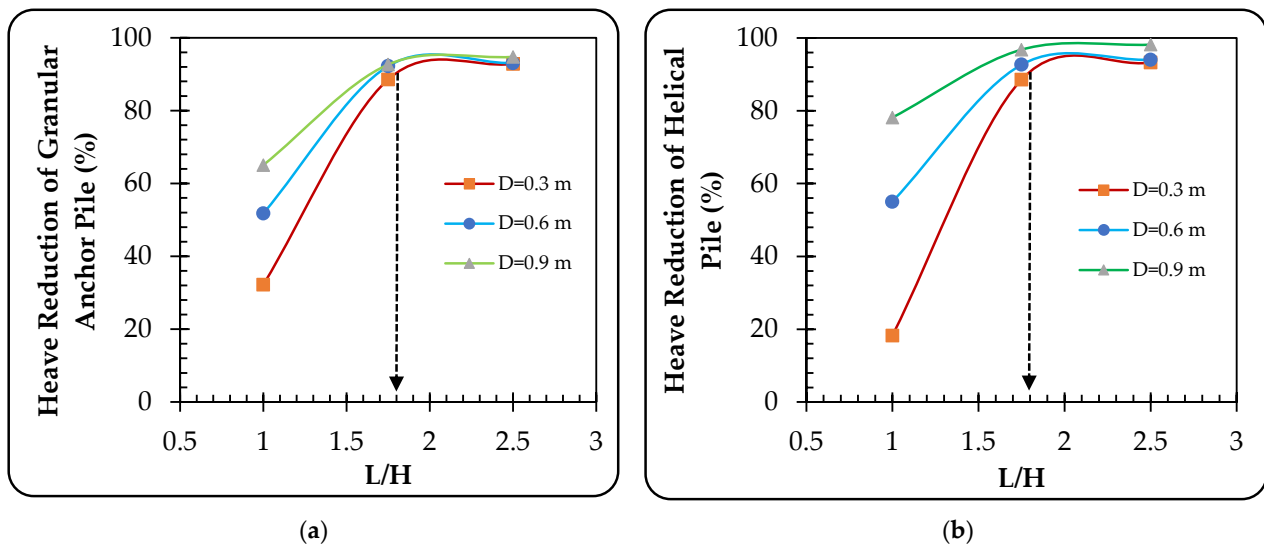
**Figure 17.** The relationship between the percentage of heave reduction and the length-to-effective zone thickness ratio (L/H) for Case 1: (a) granular anchor piles, (b) helical piles.

Figure 18 illustrates the relationship between heave reduction and pile diameter for various lengths. The findings indicate that increasing the pile diameter leads to a noticeable decrease in heave when the pile is situated within the active zone. However, for longer pile lengths and penetration into the stable zone, the diameter plays a less decisive role in heave reduction. In such cases, the heave reduction percentage steadily increases with diameter.

In summary, the behavior of piles subjected to saturation from the top is strongly influenced by the pile diameter. Helical piles exhibit superior performance compared to granular piles when the diameter is increased. The findings emphasize the substantial reduction in uplift achieved when piles penetrate the stable layer and underscore the significance of pile length and diameter in achieving uplift reduction. These insights contribute to a better understanding of pile behavior under saturation conditions, and they can assist in optimizing pile design for specific soil conditions.

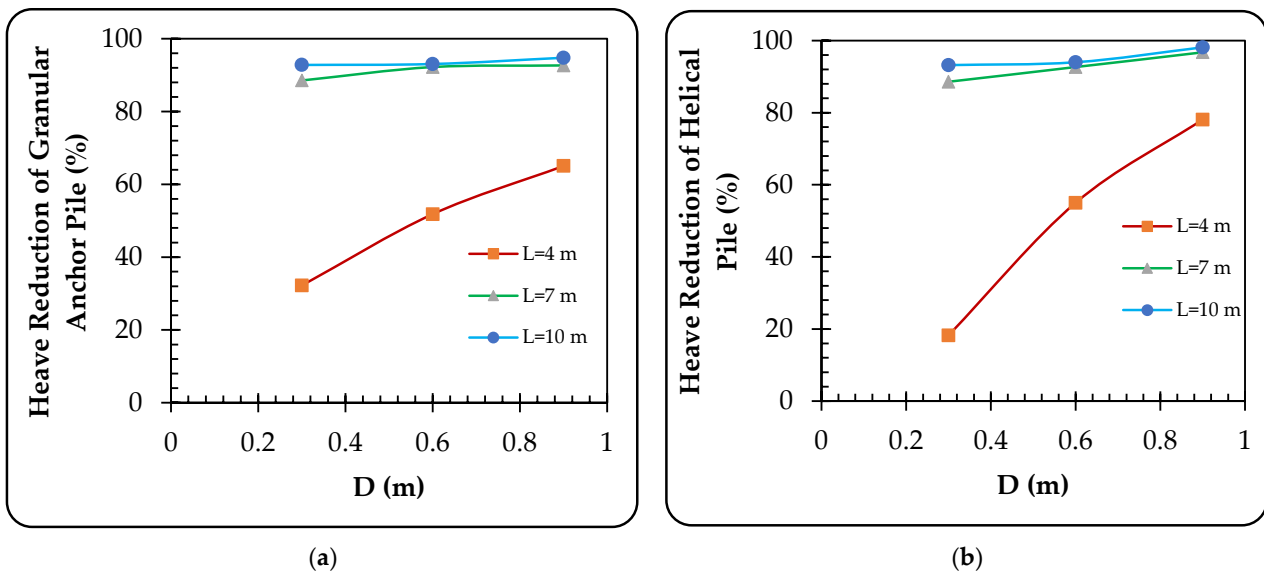
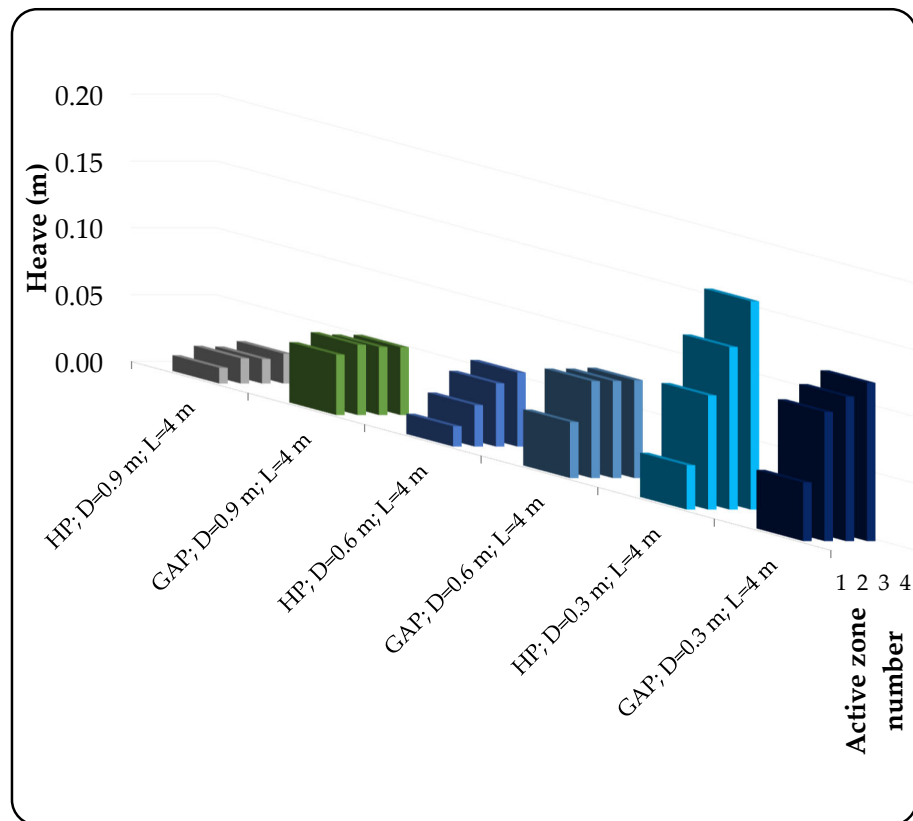


Figure 18. The relationship between the percentage of heave reduction and pile diameter for different pile lengths in Case 1: (a) granular anchor piles, (b) helical piles.

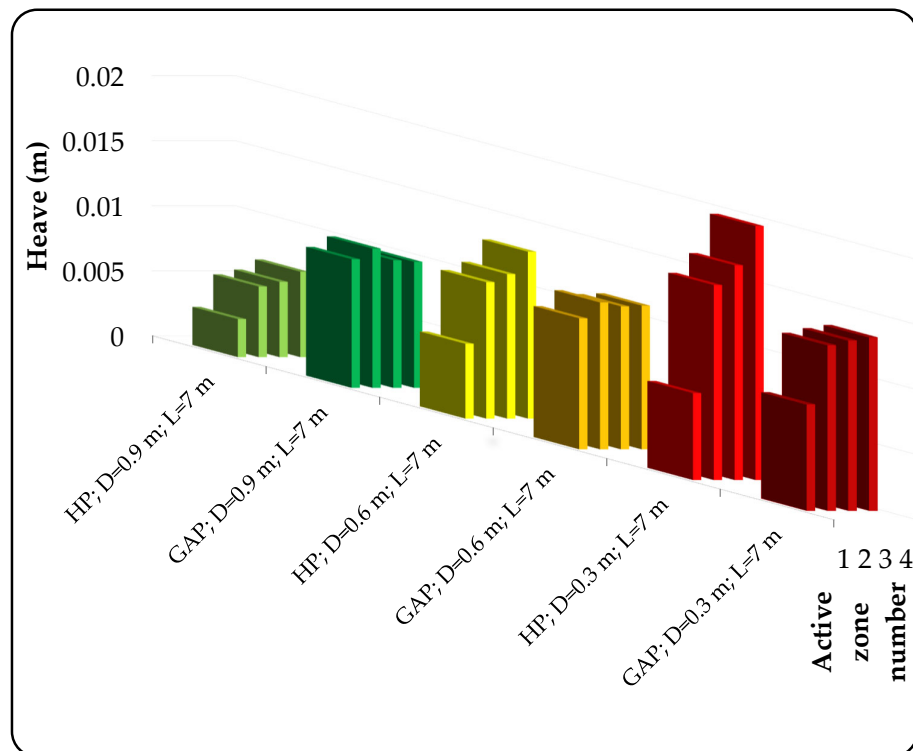
Starting Saturation from the Bottom of Active Soil (Case 2)

For this case, as shown in Figure 18 and similar to the saturation starting from the top, both an increase in pile diameter and length contribute to heave reduction. Increasing the diameter for the same length favors the superiority of helical piles over granular piles. This can be attributed to the disruptive nature of helical pile installation, which leads to the disturbance of expansive soil and subsequently reduces its swelling capacity. In contrast, increasing the diameter of granular piles enhances the lateral area, thereby increasing their interaction with the expansive soil and the resulting forces exerted on the pile due to saturation. It was also observed that penetration of the piles into the stable zone significantly reduces heave for both types of piles. The confinement stresses increase, resulting in higher frictional resistance to swelling. Furthermore, increasing the confinement stresses with depth provides a more secure anchorage for helical piles. The behavior is consistent with the findings of Muthukumar and Shukla [40], albeit with some minor differences due to the smaller scale of their tests.

It is worth mentioning that the behavior of granular anchor piles during saturation from the bottom differs from that of helical piles. Figure 19 illustrates a fundamental difference between the two pile types. As initial saturation occurs, the granular pile experiences a reduction in resistance while the helical pile maintains its resistance. This can be attributed to the presence of granular soil, which plays an active role after the saturation of the first and second zones. It negatively affects the increase in heave resulting from the saturation of Zones 1 and 2 due to the increased friction at these depths caused by the close interaction between granular soil and expansive soil. Table 8 presents the heave reduction ratios for both helical and granular anchor piles compared to the case of unreinforced soil. The table shows that the heave reduction values are closely approximated when the pile penetrates the stable layer. However, when the pile is fully located within the active zone ($L = 4$ m) and has a small diameter ($D = 0.3$ m), a similar pattern to the saturation from the top is observed, where the performance of the granular pile surpasses that of helical piles. With increasing diameter, the helical pile regains its superiority over granular piles.



(a)



(b)

Figure 19. Cont.

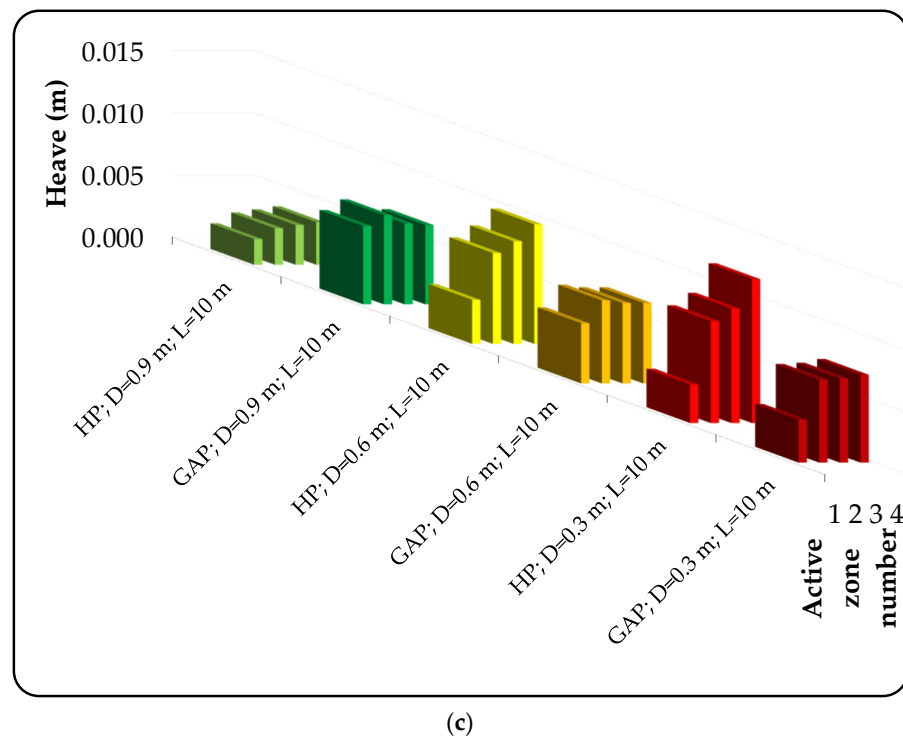


Figure 19. Heave behavior at different diameters of helical and granular anchor piles for Case 2. (a) $L = 4$ m, (b) $L = 7$ m, (c) $L = 10$ m.

Table 8. Heave reduction percentages for both helical piles and granular anchor piles compared to the unreinforced soil case in Case 2.

D (m)	L (m)	Reduction Heave of Granular Anchor Pile (%)			Reduction Heave of Helical Pile (%)		
		4	7	10	4	7	10
0.3		54.38	94.87	97.27	39.96	92.49	95.53
0.6		71.78	95.75	97.05	78.66	95.07	96.29
0.9		80.46	96.27	97.54	91.38	97.47	98.68

Figure 20 highlights the importance of penetration within the stable zone and illustrates the relationship between the heave reduction ratio and the ratio of pile length to effective zone thickness in Case 2. The figure demonstrates that increasing the length significantly reduces heave. To achieve a heave reduction ratio of 90%, having L/H not less than 1.8 is preferable, i.e., $L/H > 1.8$, which aligns with the findings for saturation starting from the top.

Furthermore, Figure 21 illustrates the relationship between the heave reduction ratio and pile diameter for various lengths in Case 2. It shows that increasing the diameter significantly reduces heave when the pile is located within the effective zone. However, as the piles penetrate into the stable zone, the diameter plays a less decisive role in heave reduction, as the heave reduction ratio only marginally increases with diameter. This finding is also consistent with the case of saturation starting from the top.

In comparing the two cases, it is observed that the final heave for Case 2 is less than that of Case 1 (see Figure 16 vs. Figure 19). Saturation from the bottom (Figure 19) results in approximately 40–80% of the heave compared to seepage from the top (Figure 16), considering different lengths and diameters.

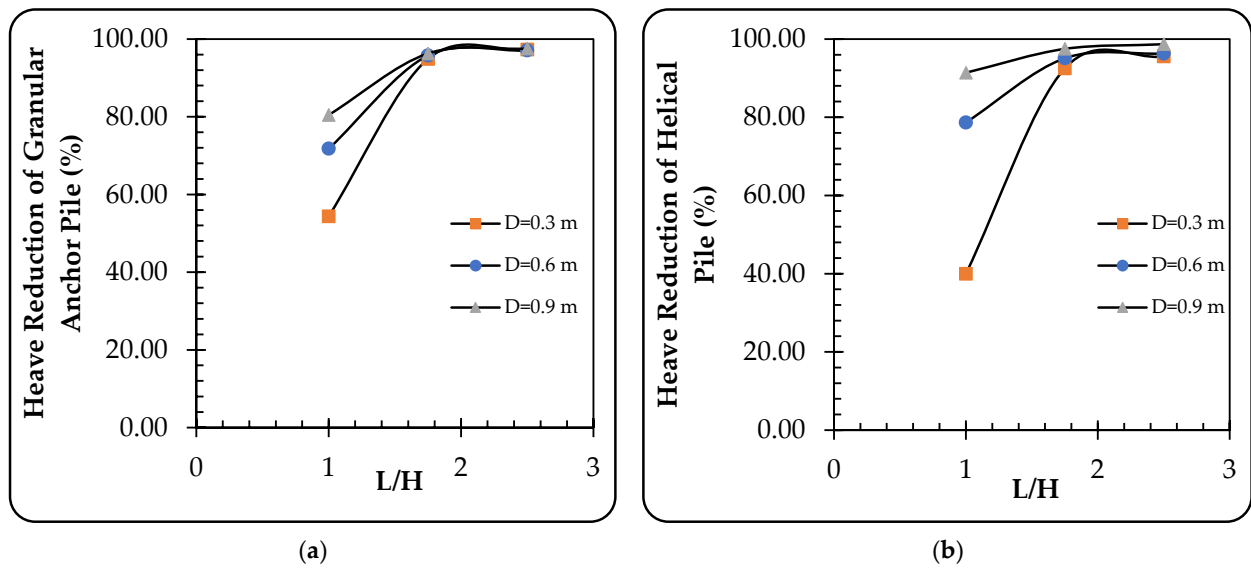


Figure 20. The relationship between percentage of heave reduction and pile length-to-effective zone thickness ratio (L/H) for Case 2: (a) granular anchor piles, (b) helical piles.

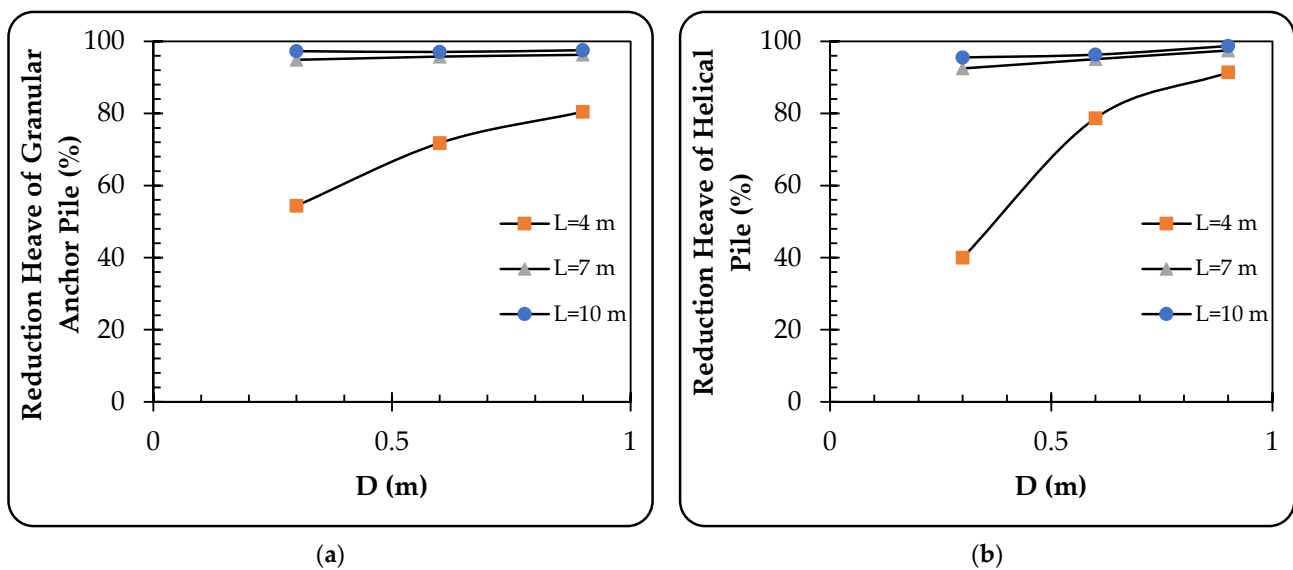


Figure 21. The relationship between heave reduction ratio and pile diameter for different pile lengths in Case 2: (a) granular anchor piles, (b) helical piles.

Therefore, saturation from the top is considered the more critical scenario. In this case, both types of piles are effective in reducing heave, and it is not preferable to use large diameters exceeding 0.6 m. Increasing the diameter does not significantly contribute to reducing heave, especially for piles that penetrate the stable layer.

These results indicate that granular piles achieve very close effectiveness in reducing heave compared to helical piles and sometimes even outperform them, particularly in the case of saturation from the bottom.

3.2. Effect of Cap Width (B)

The influence of cap width on both pullout and compressive bearing capacities, as well as its impact on the corresponding heave values, was investigated. The diameters and the lengths of both helical and granular anchor piles were consistently set at 0.6 m and 7 m, respectively. Three different values of cap width were considered: 1, 2, and 4 m.

It is well established that an increase in the cap width has a notable effect on enhancing both the pullout and the compressive bearing capacities of the pile. This effect can be attributed to the increased contact surface area and adhesion with the underlying expansive soil. Furthermore, the added weight of the wider cap contributes to an amplified pullout force, while the enlarged dimensions of the failure surface in the soil lead to increased compressive force. Regarding heave, an increased cap width has a significant impact on elevating the heave values. This can be attributed to the larger contact surface area between the pile cap and the expansive soil, resulting in higher applied swelling pressures due to saturation, as illustrated in Figure 22.

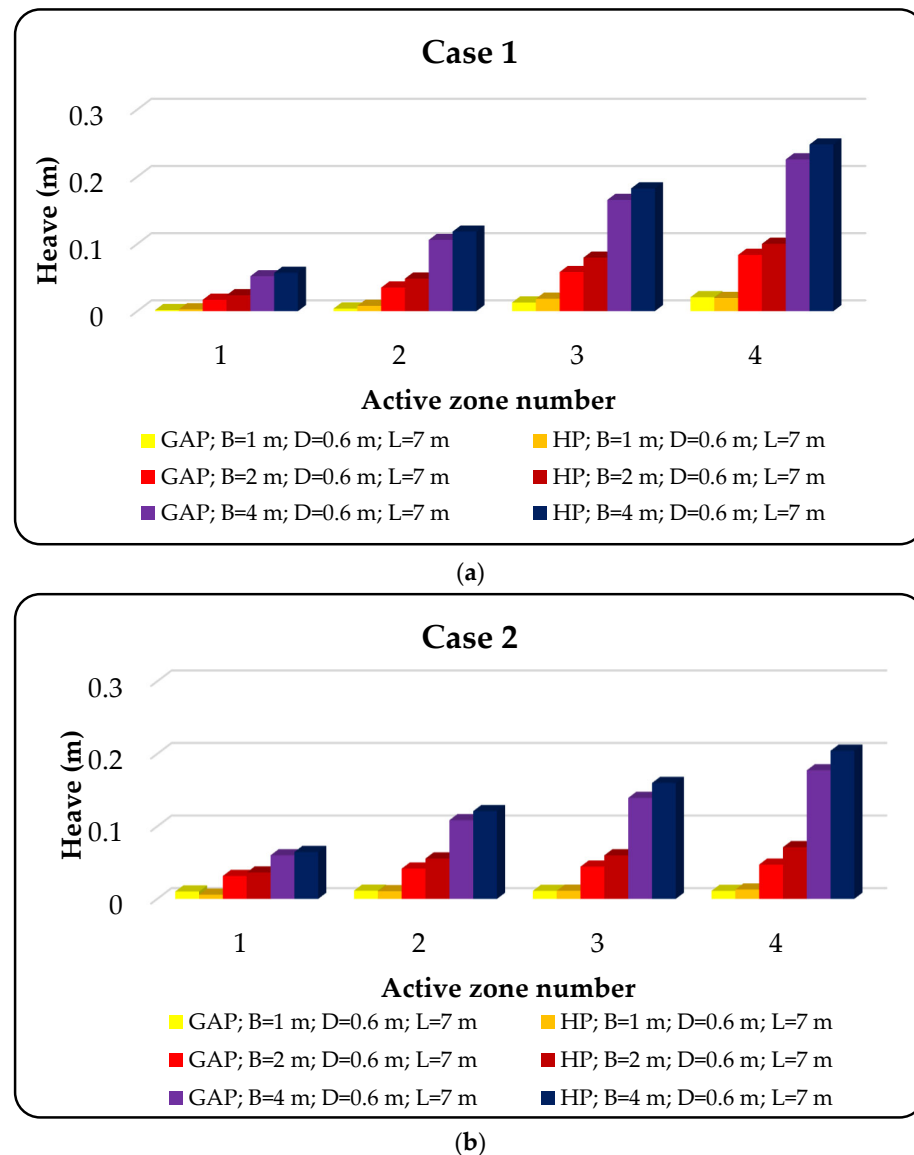


Figure 22. Effect of increased cap width on the heave of helical and granular anchor piles; (a) Case 1, (b) Case 2.

To address the challenge of significant heave associated with the use of large-sized pile caps or mats, a potential strategy is to elevate these caps above the expansive soil (referred to as a high-rise pile cap). This approach aims to mitigate the observed heave. The subsequent section provides a comprehensive examination of this methodology.

3.3. High-Rise Pile Cap

The pile cap was elevated above the expansive soil by half a meter. Three different diameters were considered: 0.3 m, 0.6 m, and 0.9 m. It was assumed that the pile had a length of 4 m, with its entire length embedded within the expansive soil. This selection was made to enhance the clarity of the behavior, as the heave of the piles with elevated caps penetrating the stable layer would be very small, making it challenging to demonstrate the behavior clearly.

3.3.1. Influence of High-Rise Pile Cap on the Pull-Out Load

Figure 23 illustrates the relationship curves depicting the response of upward movement and the pull-out load for helical and granular anchor piles under the influence of high-rise pile caps. The numerical results reveal that an increase in the diameter of the pile leads to a corresponding augmentation in the pull-out load. Particularly, the granular anchor piles exhibit a notably higher pull-out capacity compared to the helical anchor piles, displaying percentage increases of 37%, 43%, and 47% for pile diameters of 0.3 m, 0.6 m, and 0.9 m, respectively. It is important to note that low-rise pile caps, which are not elevated, can offer even greater uplift capacities. This enhanced performance can be attributed to the adhesive forces established between the pile cap and the underlying expansive soil. However, if the adhesive forces are disregarded, the uplift capacity remains unchanged for both high-rise and low-rise pile cap configurations.

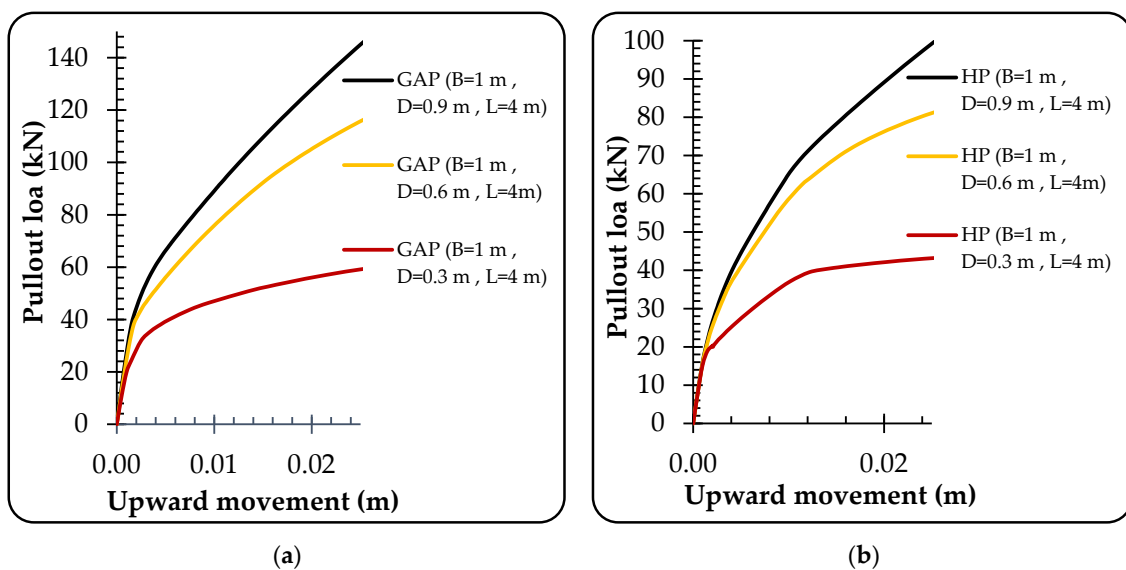


Figure 23. Relationship curves between upward movement and pull-out load for helical and granular anchor piles in the case of high-rise pile caps: (a) granular anchor piles, (b) helical piles.

3.3.2. Effect of High-Rise Pile Cap on the Compressive Load

The compressive load behavior of helical and granular anchor piles in the presence of high-rise pile caps and low-rise pile caps is investigated in Figure 24. The curves illustrate the relationship between the downward movement and the compressive load for both types of anchor piles under different pile cap configurations. As the diameter of the piles increases, the compressive load capacity of high-rise pile caps for both helical and granular anchor piles shows improvement, reaching its maximum at a diameter of 0.6 m. However, beyond this diameter, the incremental enhancement becomes negligible.

An important finding is a remarkable convergence in the load-bearing capacities under compressive load for helical and granular anchor piles with high-rise pile caps in expansive soil conditions. This convergence can be attributed to the direct transmission of applied loads from the pile cap to the bearing zone located at the bottom of the pile, particularly through the plate helix. The limited contribution of the shaft section in high-rise pile caps,

characterized by its small size and insufficient resistance to bear substantial loads through friction with the surrounding soil, reinforces this direct load transfer mechanism.

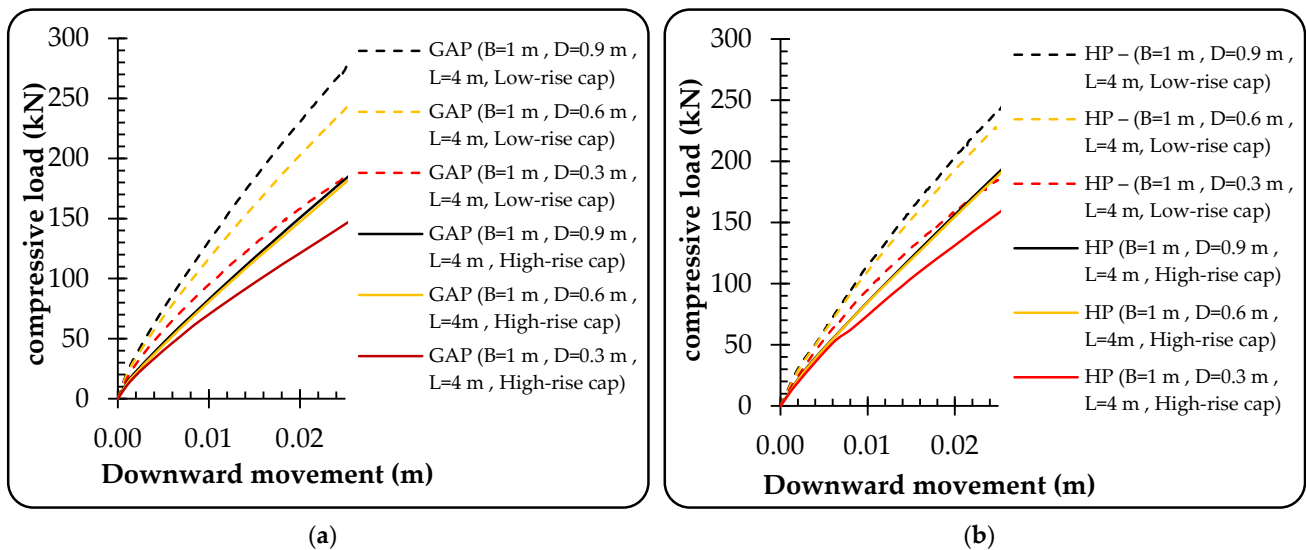


Figure 24. Relationship curves between downward movement and compressive load for helical and granular anchor piles in the cases of high-rise pile caps and low-rise pile caps: (a) granular anchor piles, (b) helical piles.

Additionally, a comparison between high-rise pile caps and low-rise pile caps reveals that the latter exhibit higher compressive load-bearing capacities. This superiority in performance can be attributed to the active participation of the expansive soil in directly supporting the loads imposed by the pile cap. The interaction between the low-rise pile cap and the expansive soil facilitates the direct transfer of loads, resulting in an enhanced load-bearing capacity.

3.3.3. Effect of High-Rise Pile Caps on Heave

The effect of high-rise pile caps on the heave behavior is investigated in Figure 25, comparing the performance of helical anchor piles and granular anchor piles under two saturation conditions: saturation from the top (Case 1) and saturation from the bottom (Case 2). In Case 1, notable differences were observed between the behavior of granular anchor piles and helical anchor piles. The granular piles exhibited upward movement (heave), while the helical piles experienced downward movement (settlement), accompanied by soil saturation. In contrast, in Case 2, both types of piles displayed similar settlement behavior with increasing saturation. These variations can be attributed to the complex interaction between the pile shaft and the disturbed soil (for helical piles) or the compacted soil (for granular piles) on the one hand and the interaction between these soils and the surrounding expansive soils on the other.

Comparing the deformations of helical and granular anchor piles, it is evident that both types demonstrate high effectiveness in mitigating deformations resulting from volumetric changes in expansive soil due to saturation. In most cases, granular anchor piles outperformed helical anchor piles in reducing deformations, except for instances involving larger diameters, such as a diameter of 0.9 m. As previously mentioned, it is advisable to avoid using diameters larger than 0.6 m for both helical and granular anchor piles, as larger diameters do not significantly contribute to heave reduction. This observation holds true when considering the influence of high-rise pile caps as well.

Comparing the high-rise pile caps, shown in Figure 25, with the low-rise pile caps depicted in Figures 16a and 18a, it becomes apparent that high-rise pile caps have a substantial effect on reducing heave. This can be attributed to the lifting of pile caps, which prevents the transmission of swell pressure loads beneath the caps, consequently

minimizing heave. High-rise cap piles primarily experience lateral pressure along the length of the pile due to soil heave, while the relatively small diameter of the pile shaft reduces the impact of frictional forces resulting from this lateral pressure, thereby mitigating the effect on pile heave.

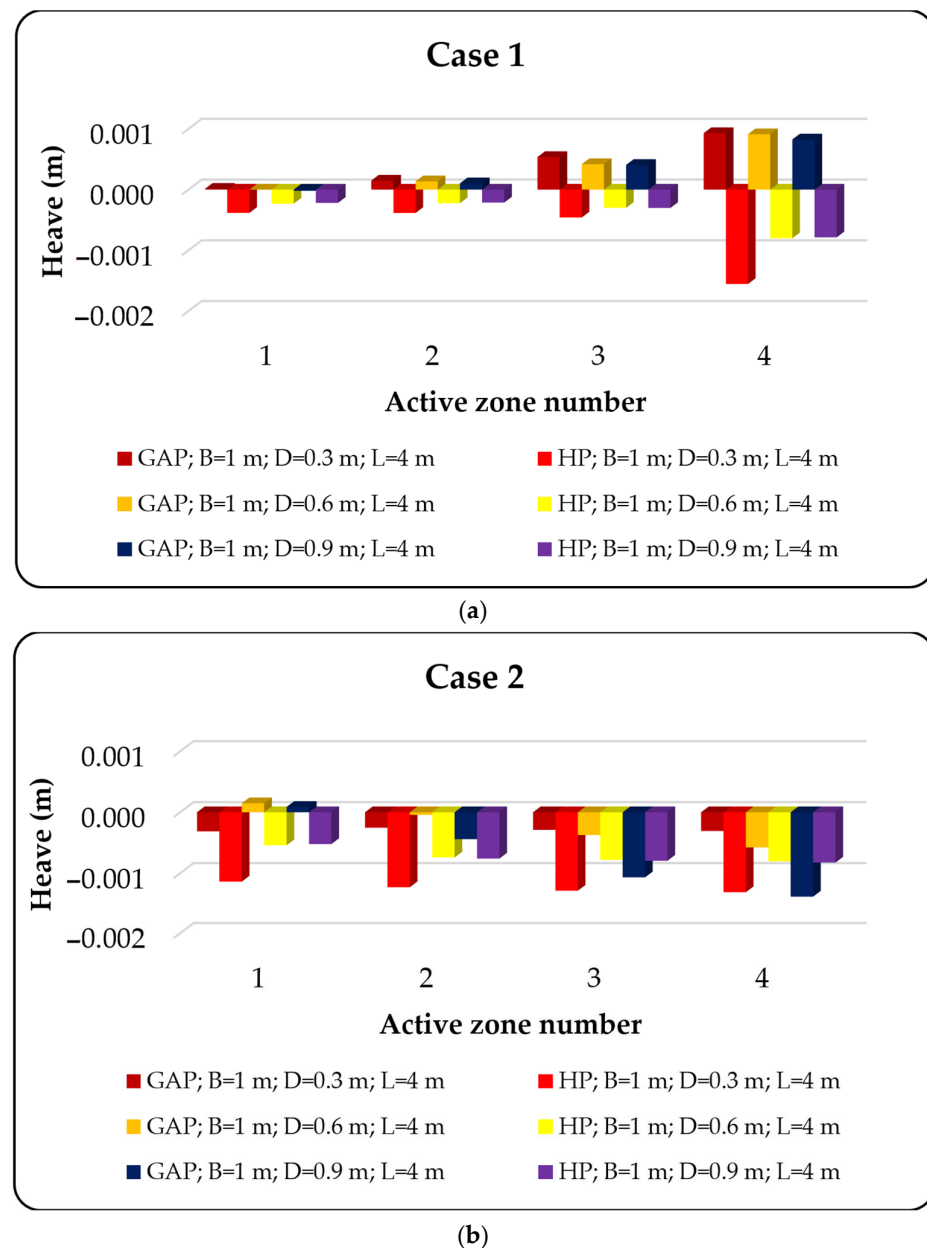


Figure 25. Comparison between helical anchor piles and granular anchor piles with high-rise pile caps in saturation conditions from the Top (Case 1) and from the Bottom (Case 2): (a) Case 1, (b) Case 2.

3.4. Effect of Relative Density of Granular Material on Granular Anchor Pile Behavior

The influence of relative density is a critical factor to consider during the construction of granular anchor piles. Previous studies demonstrated that increasing the relative density contributes to improved behavior and load-bearing capacity of these piles [39,43]. However, most of these studies were limited to small-scale laboratory tests and did not specifically investigate the impact on heave behavior. As a result, this study explores three different relative densities: 35%, 65%, and 90%, representing loose, medium, and dense granular soils, respectively. Detailed specifications for these relative densities can be found in Table 9.

Table 9. Properties of granular soil used to study the effect of relative density.

	Dr = 35%	Dr = 65%	Dr = 90%
γ_{unsat} (kN/m ³)	15	16.5	19
γ_{sat} (kN/m ³)	17.5	18.5	21
E_{50}^{ref} (kN/m ²)	20,000	35,000	50,000
E_{oed}^{ref} (kN/m ²)	20,000	35,000	50,000
E_{ur}^{ref} (kN/m ²)	60,000	105,000	150,000
C' (kN/m ²)	0.1	0.1	0.1
ϕ' (°)	30	36	38
Ψ (°)	0	6	8
ν_{ur} (–)	0.2	0.2	0.2
m (–)	0.5	0.5	0.5

The investigation utilized 0.6 m diameter piles, and two different lengths were examined: 4 m, representing full embedding of the pile within the expansive soil, and 7 m, with the pile penetrating the stable layer by 3 m. The subsequent sections provide a comprehensive analysis of the influence of relative density on pullout loads, compressive loads, and the magnitude of heave.

3.4.1. Influence of Relative Density of Granular Material on the Pullout Load

Figure 26 illustrates the relationship between the pullout load and the upward movement for pile lengths of 4 and 7 m, corresponding to different relative densities. Increasing the relative density results in higher upward load capacity, corresponding to a 25 mm movement, by 19% and 24% for pile lengths of 4 and 7 m, respectively. This can be attributed to the increase in frictional forces and the enhanced interaction between different contact surfaces, leading to improved pullout load capacity.

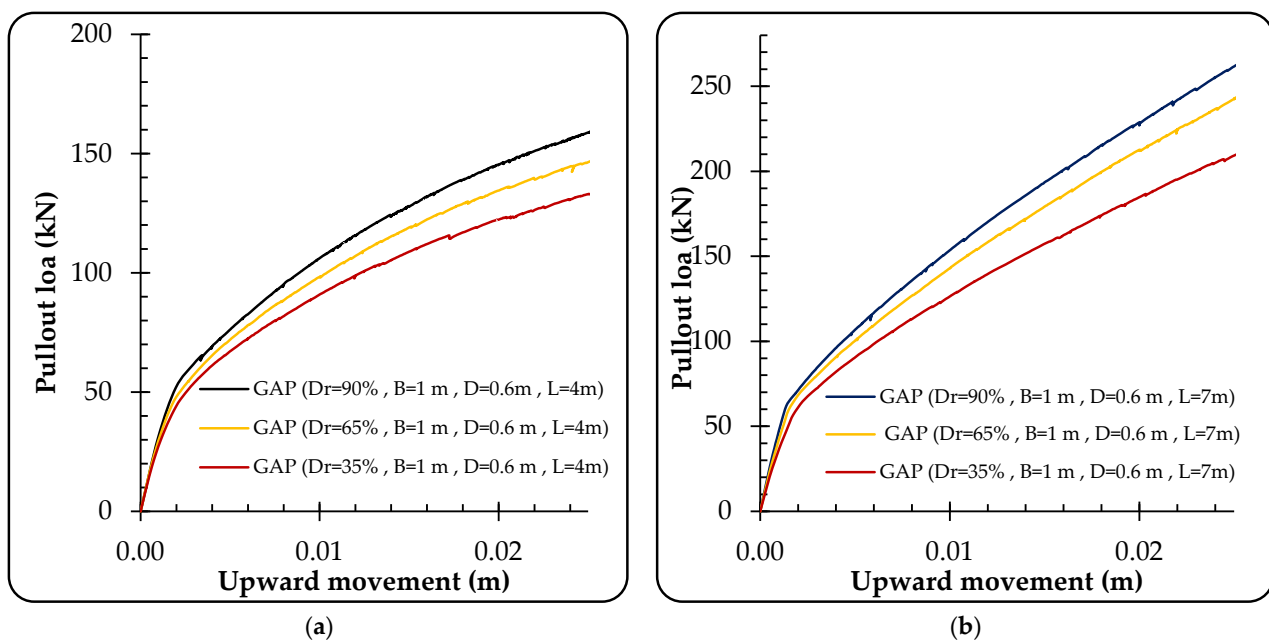


Figure 26. Relationship curves between pullout load and upward movement for pile lengths of 4 and 7 m under different relative densities: (a) L = 4 m, (b) L = 7 m.

The higher relative density promotes better particle interlocking and densification within the granular material, resulting in increased resistance to upward movement. The increased contact area and the stronger inter-particle friction contribute to the improved load-bearing capacity of the piles, thus reducing the upward movement under the applied load.

3.4.2. Effect of Relative Density of Granular Material on the Compressive Load

Figure 27 illustrates the relationship curves between the compressive load and the downward movement for pile lengths of 4 and 7 m under varying relative densities. The compressive load represents the resistance required to induce a downward displacement of 25 mm.

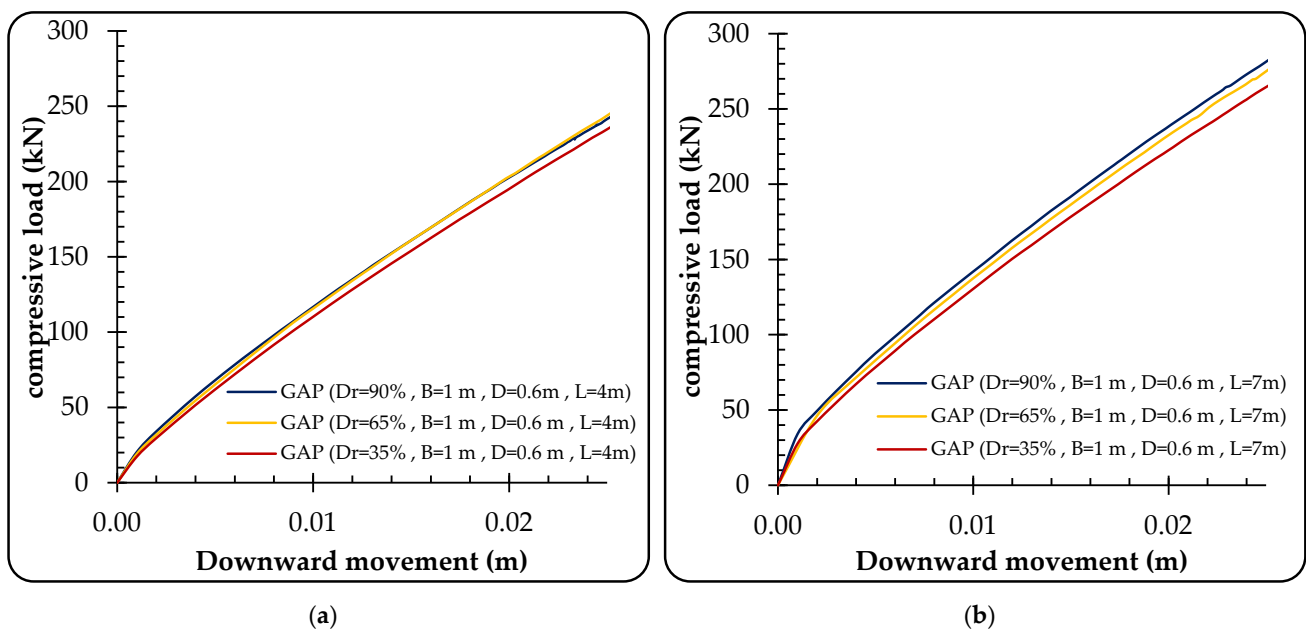


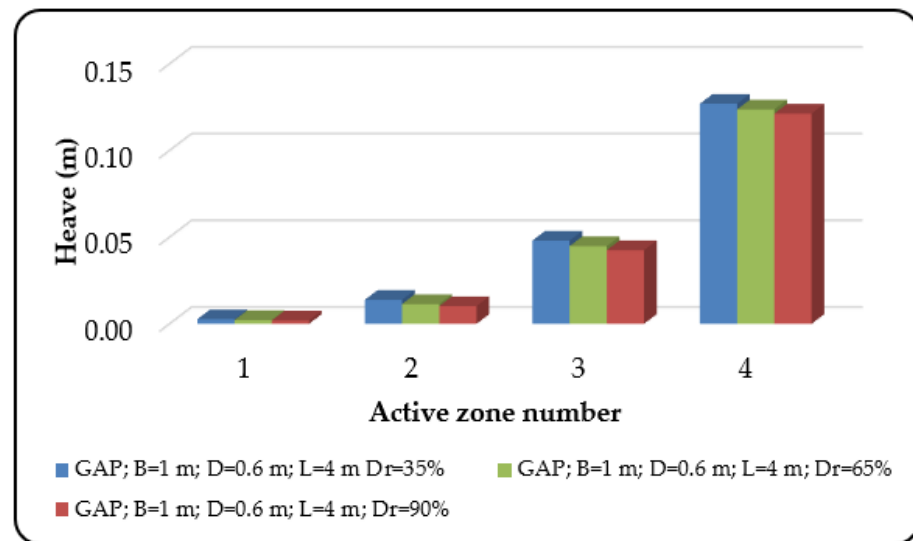
Figure 27. Relationship curves between compressive load and downward movement for pile lengths of 4 and 7 m under varying relative densities: (a) $L = 4$ m, (b) $L = 7$ m.

The results indicate that increasing the relative density of the granular material leads to a slight increase in the corresponding compressive load for both 4 m and 7 m pile lengths. Specifically, the compressive load shows a marginal increment of 3% and 6.4% for the respective pile lengths.

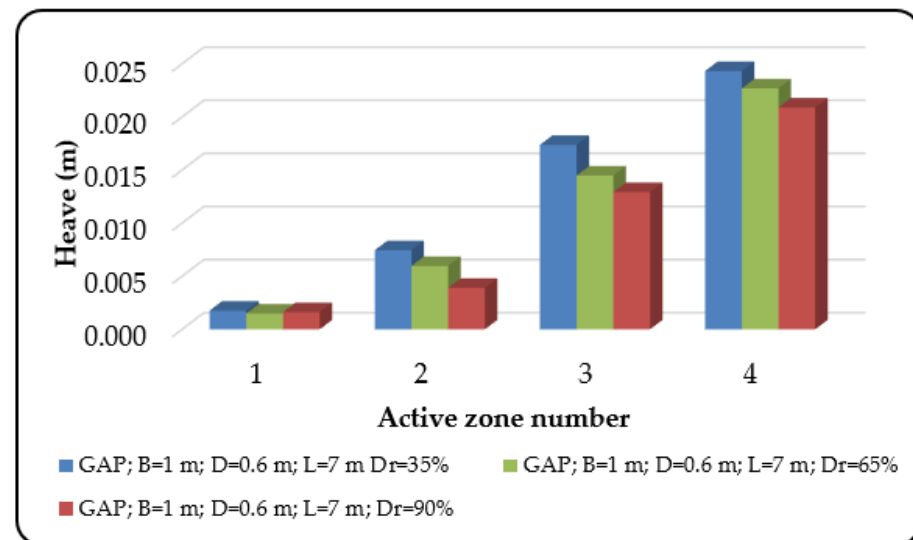
However, it is important to note that the influence of relative density on increasing the compressive load is relatively insignificant compared to its impact on the uplift load. This suggests that the primary effect of relative density lies in its ability to enhance the load-bearing capacity and mitigate the upward movement rather than significantly impacting the compressive load.

3.4.3. Effect of Relative Density of Granular Material on the Heave Starting Saturation from the Top (Case 1)

Figure 28 illustrates the variations in heave for the pile lengths of 4 and 7 m under different relative densities for Case 1, where saturation starts from the top. Increasing the relative density from 35% to 90% reduces the heave by a small margin, approximately 5% and 14% for the pile lengths of 4 and 7 m, respectively. Thus, the effect of relative density on the heave reduction becomes more effective when there is sufficient embedment within the stable layer, as the higher relative density enhances the anchorage of the pile within the stable soil.



(a)



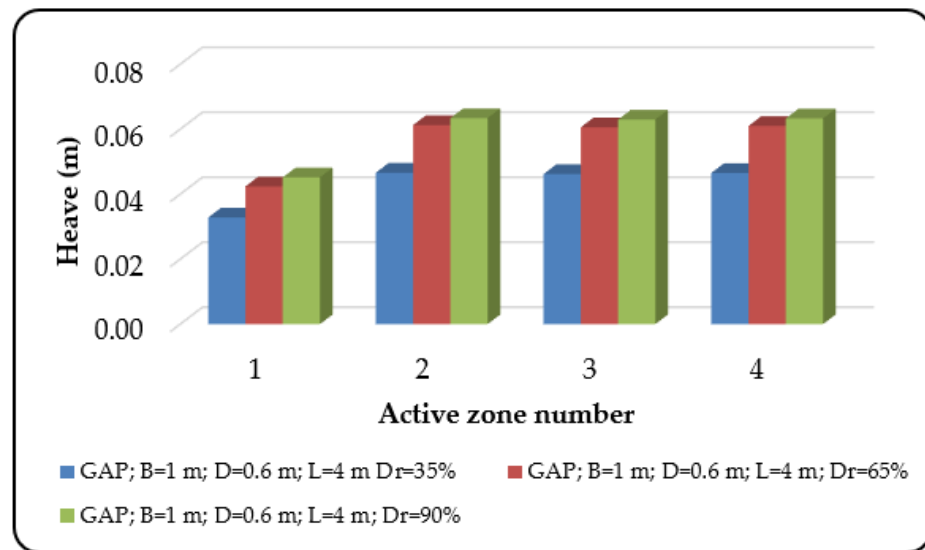
(b)

Figure 28. Variations in heave for pile lengths of 4 and 7 m under different relative densities for Case 1: (a) $L = 4$ m, (b) $L = 7$ m.

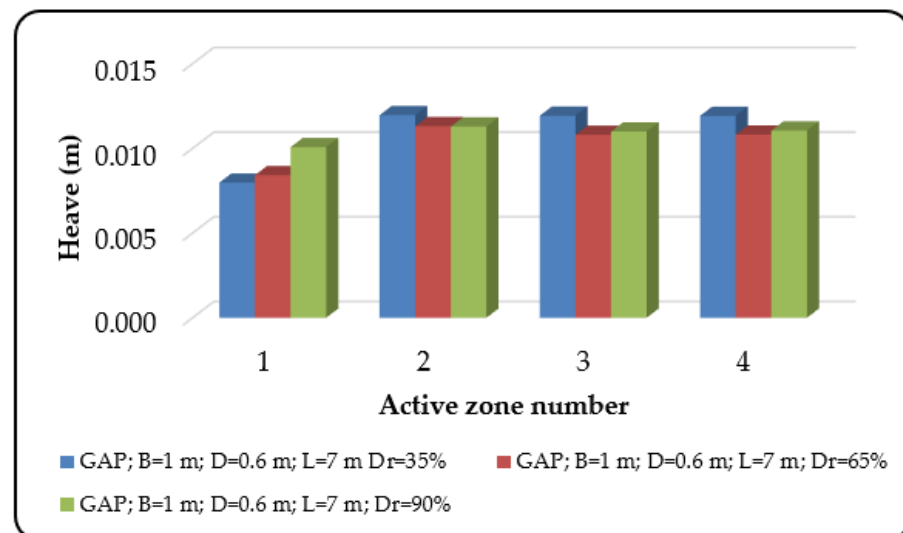
Starting Saturation from the Bottom of Active Soil (Case 2)

Figure 29 illustrates the changes in heave for the pile lengths of 4 and 7 m under different relative densities for Case 2. It was observed that increasing the relative density has a negative effect when the pile is fully embedded within the expansive soil, as it leads to an approximately 35% increase in heave when the relative density increases from 35% to 90%. However, in the presence of sufficient embedment depth, increasing the relative density reduces the magnitude of heave during full saturation of the expansive layer.

When comparing Cases 1 and 2, it is recommended to use higher relative densities when there is a significant embedment depth. On the other hand, when the pile is fully embedded within the expansive soil, it is not advisable to utilize high relative densities. This is because high relative densities enhance the interaction between the pile and the expansive soil, resulting in increased pile heave.



(a)



(b)

Figure 29. Variations in heave for pile lengths of 4 and 7 m under different relative densities for Case 2: (a) $L = 4$ m, (b) $L = 7$ m.

4. Conclusions

The objectives of this study were to evaluate the performance of granular anchor piles (GAP) and helical piles (HP) in expansive soils using Plaxis 3D simulation. The major findings are as follows:

1. Comparative Performance of Anchor Techniques:
 - GAP outperformed HP in pullout and compressive load resistance, with improvements of 17–22.5% and 0.5–19%, respectively, depending on the specific pile length and diameters examined.
 - Both GAP and HP were effective in reducing heave, with reductions exceeding 90% under certain conditions.
 - High-rise cap piles exhibited significant reductions in heave compared to low-rise cap piles.
2. Influence of Length, Diameter, and Cap Width:
 - Increasing pile length improved pullout and compressive load resistance.

- Enlarging pile diameter enhanced frictional resistance, but beyond 0.6 m, further increases had diminishing returns.
 - Increasing cap width improved pullout and compressive bearing capacities but led to elevated heave. To address the challenge of significant heave associated with large-sized pile caps or mats, a potential strategy involves elevating these caps above the expansive soil, known as a high-rise pile cap.
3. Influence of Relative Density:
- Higher relative density of the granular material increased upward load capacity, with observed increases of 19% and 24% in 25 mm movement for pile lengths of 4 m and 7 m, respectively.
 - Higher relative density slightly improved compressive load for both 4 m and 7 m pile lengths. The compressive load demonstrated marginal increments of 3% and 6.4% for the respective pile lengths.
 - Higher relative densities are recommended for significant embedment depth.

This study provides a comprehensive evaluation of GAP and HP performance in expansive soils. The analysis considered multiple parameters and their impact on load resistance and heave behavior. The findings provide crucial insights into the suitability and performance of these techniques for stabilizing foundations on expansive soils. Future studies can consider soil moisture content, temperature effects, and advanced modeling techniques. Conducting field tests will be crucial in validating the numerical findings and enhancing the applicability of the results. Furthermore, future research endeavors should consider the implementation of advanced modeling techniques and address sustainability aspects in the design and application of these pile techniques.

Author Contributions: Conceptualization, A.A. and R.P.R.; investigation, A.A.; writing—original draft preparation, A.A.; numerical modeling, A.A., R.P.R. and R.A.; writing—review and editing, A.A.; supervision, R.P.R. All authors have read and agreed to the published version of the manuscript.

Funding: This research received no external funding.

Informed Consent Statement: Not applicable.

Conflicts of Interest: The authors declare no conflict of interest.

References

1. Stoll, S.C.; Henning, S.R.; Bagley, A.D.; Wiegand, K.T. Foundation Damage Assessments and Structural Repairs. In *Forensic Engineering*; American Society of Civil Engineers: Denver, CO, USA, 2022; pp. 166–174, ISBN 9780784484548.
2. Baer, D.H. *Building Losses from Natural Hazards: Yesterday, Today and Tomorrow*; JH Wiggins Co.: Redondo Beach, CA, USA, 1978.
3. Devkota, B.; Karim, M.R.; Rahman, M.M.; Nguyen, H.B.K. Accounting for Expansive Soil Movement in Geotechnical Design—A State-of-the-Art Review. *Sustainability* **2022**, *14*, 15662. [[CrossRef](#)]
4. Bowles, J.E. *Foundation Analysis and Design*; McGraw-Hills Inc.: New York, NY, USA, 1988; ISBN 0070067767.
5. McOmber, R.M.; Thompson, R.W. Verification of Depth of Wetting for Potential Heave Calculations. In *Advances in Unsaturated Geotechnics*; ASCE: Reston, VA, USA, 2000; pp. 409–422.
6. Nelson, J.D.; Overton, D.D.; Durkee, D.B. Depth of Wetting and the Active Zone. In *Expansive Clay Soils and Vegetative Influence on Shallow Foundations*; ASCE: Reston, VA, USA, 2001; pp. 95–109.
7. Walsh, K.D.; Colby, C.A.; Houston, W.N.; Houston, S.L. Method for Evaluation of Depth of Wetting in Residential Areas. *J. Geotech. Geoenviron. Eng.* **2009**, *135*, 169–176. [[CrossRef](#)]
8. Teodosio, B.; Kristombu Baduge, K.S.; Mendis, P. A Review and Comparison of Design Methods for Raft Substructures on Expansive Soils. *J. Build. Eng.* **2021**, *41*, 102737. [[CrossRef](#)]
9. Ijaz, N.; Ye, W.; ur Rehman, Z.; Dai, F.; Ijaz, Z. Numerical Study on Stability of Lignosulphonate-Based Stabilized Surficial Layer of Unsaturated Expansive Soil Slope Considering Hydro-Mechanical Effect. *Transp. Geotech.* **2022**, *32*, 100697. [[CrossRef](#)]
10. Fulzele, U.G.; Ghane, V.R.; Parkhe, D.D. Study of Structures in Black Cotton Soil. In Proceedings of the IRF International Conference on Advances Sciences Engineering & Technology, Pune, India, 16 October 2016; Volume 4, ISBN 978-93-86291-14-1.
11. Zamin, B.; Nasir, H.; Mehmood, K.; Iqbal, Q. Field-Obtained Soil-Water Characteristic Curves of KPK Expansive Soil and Their Prediction Correlations. *Adv. Civ. Eng.* **2020**, *2020*, 4039134. [[CrossRef](#)]
12. Dang, L.C.; Khabbaz, H.; Ni, B.J. Improving Engineering Characteristics of Expansive Soils Using Industry Waste as a Sustainable Application for Reuse of Bagasse Ash. *Transp. Geotech.* **2021**, *31*, 100637. [[CrossRef](#)]

13. Medina-Martinez, C.J.; Sandoval-Herazo, L.C.; Zamora-Castro, S.A.; Vivar-Ocampo, R.; Reyes-Gonzalez, D. Natural Fibers: An Alternative for the Reinforcement of Expansive Soils. *Sustainability* **2022**, *14*, 9275. [[CrossRef](#)]
14. Taleb, T.; Unsever, Y.S. Study on Strength and Swell Behavioral Change and Properties of the Clay—Fiber Mixtures. *Sustainability* **2022**, *14*, 6767. [[CrossRef](#)]
15. Tiwari, N.; Satyam, N.; Puppala, A.J. Effect of Synthetic Geotextile on Stabilization of Expansive Subgrades: Experimental Study. *J. Mater. Civ. Eng.* **2021**, *33*, 04021273. [[CrossRef](#)]
16. Tiwari, N.; Satyam, N. Coupling Effect of Pond Ash and Polypropylene Fiber on Strength and Durability of Expansive Soil Subgrades: An Integrated Experimental and Machine Learning Approach. *J. Rock Mech. Geotech. Eng.* **2021**, *13*, 1101–1112. [[CrossRef](#)]
17. Tiwari, N.; Satyam, N.; Puppala, A.J. Strength and Durability Assessment of Expansive Soil Stabilized with Recycled Ash and Natural Fibers. *Transp. Geotech.* **2021**, *29*, 100556. [[CrossRef](#)]
18. Li, H.; Wang, Y.; Yin, Z.; Al-Soudani, W.H.S.; Fattah, M.Y.; Ziyara, H.M.; Albusoda, B.S. An Experimental Study of the Load Carrying Capacity of Straight Shaft and Underreamed Piles in Expansive Soil. *IOP Conf. Ser. Mater. Sci. Eng.* **2021**, *1067*, 012050. [[CrossRef](#)]
19. Onur, M.İ.; Bıçakçı, M.; Kardoğan, P.S.Ö.; Erdağ, A.; Aghlmand, M. Laboratory Model Design for Deep Soil Mixing Method. *Adv. Civ. Archit. Eng.* **2022**, *13*, 59–69. [[CrossRef](#)]
20. El-Samea, A.; Hassan, W.; Mowafy, Y.M.; El-Naiem, A.; Abdo, M.; Towfeek, A.R. Numerical Analysis of Shallow Foundation on Expansive Soil. *J. Al Azhar Univ. Eng. Sect.* **2022**, *17*, 480–501. [[CrossRef](#)]
21. Mansour, M.A.; El Naggar, M.H. Optimization of Grouting Method and Axial Performance of Pressure-Grouted Helical Piles. *Can. Geotech. J.* **2021**, *59*, 702–714. [[CrossRef](#)]
22. Ziyara, H.M.; Albusoda, B.S. Experimental and Numerical Study of the Bulb’s Location Effect on the Behavior of under-Reamed Pile in Expansive Soil. *J. Mech. Behav. Mater.* **2022**, *31*, 90–97. [[CrossRef](#)]
23. Roy, R.; Rao, C.N.; Mouli, S.S. Evaluation of Heave Behavior by Numerical Modeling of Granular Pile Anchor in Expansive Soil. *Lect. Notes Civ. Eng.* **2023**, *297*, 103–115.
24. Department of the Army USA Technical Manual. TM 5–818–7, Foundations in Expansive Soils 1983. Available online: https://armypubs.army.mil/epubs/DR_pubs/DR_a/pdf/web/tm5_818_7.pdf (accessed on 30 December 2022).
25. Das, B.M.; Shukla, S.K. *Earth Anchors*, 2nd ed.; J. Ross Publishing: Plantation, FL, USA, 2013; ISBN 978-1-60427-077-8.
26. Li, W. Centrifuge Modeling and Large Deformation Analyses of Axially Loaded Helical Piles in Cohesive Soils. Ph.D. Thesis, University of Alberta, Edmonton, AB, Canada, 2022.
27. Venkatesan, V.; Mayakrishnan, M. Behavior of Mono Helical Pile Foundation in Clays under Combined Uplift and Lateral Loading Conditions. *Appl. Sci.* **2022**, *12*, 6827. [[CrossRef](#)]
28. Malhotra, H.; Sanjay; Singh, K. Effect of Load Inclination on the Uplift Capacity of the Granular Anchor Pile Foundation in Cohesive Soil. *Arab. J. Geosci.* **2022**, *15*, 1088. [[CrossRef](#)]
29. Yu, H.; Zhou, H.; Sheil, B.; Liu, H. Finite Element Modelling of Helical Pile Installation and Its Influence on Uplift Capacity in Strain Softening Clay. *Can. Geotech. J.* **2022**, *59*, 2050–2066. [[CrossRef](#)]
30. Aljorany, A.N.; Ibrahim, S.F.; Al-Adly, A.I. Heave Behavior of Granular Pile Anchor-Foundation System (GPA-Foundation System) in Expansive Soil. *J. Eng.* **2014**, *20*, 213–222. [[CrossRef](#)]
31. Rao, A.S.; Phanikumar, B.R.; Babu, R.D.; Suresh, K. Pullout Behavior of Granular Pile-Anchors in Expansive Clay Beds in Situ. *J. Geotech. Geoenvironmental Eng.* **2007**, *133*, 531–538. [[CrossRef](#)]
32. Phanikumar, B.R.; Srirama Rao, A.; Suresh, K. Field Behaviour of Granular Pile-Anchors in Expansive Soils. *Proc. Inst. Civ. Eng. Ground Improv.* **2008**, *161*, 199–206. [[CrossRef](#)]
33. Phanikumar, B.R.; Sharma, R.S.; Rao, A.S.; Madhav, M.R. Granular Pile Anchor Foundation (GPAF) System for Improving the Engineering Behavior of Expansive Clay Beds. *Geotech. Test. J.* **2004**, *27*, 279–287. [[CrossRef](#)]
34. Vashishtha, H.R.; Sawant, V.A. An Experimental Investigation for Pullout Response of a Single Granular Pile Anchor in Clayey Soil. *Int. J. Geo. Eng.* **2021**, *12*, 35. [[CrossRef](#)]
35. Srirama Rao, A.; Phanikumar, B.R.; Suresh, K. Response of Granular Pile-Anchors under Compression. *Proc. Inst. Civ. Eng. Ground Improv.* **2008**, *161*, 121–129. [[CrossRef](#)]
36. Ismail, M.; Shahin, M. Finite Element Analyses of Granular Pile Anchors as a Foundation Option for Reactive Soils. In Proceedings of the International Conference on Advances in Geotechnical Engineering, Perth, Australia, 7–9 November 2011; Australian Geomechanics Society: Perth, Australia, 2011; pp. 1047–1052.
37. Sivakumar, V.; O’Kelly, B.C.; Madhav, M.R.; Moorhead, C.; Rankin, B. Granular Anchors under Vertical Loading—Axial Pull. *Can. Geotech. J.* **2013**, *50*, 123–132. [[CrossRef](#)]
38. Krishna, P.H.; Murty, V.R. Pull-out Capacity of Granular Anchor Piles in Expansive Soils. *IOSR J. Mech. Civ. Eng.* **2013**, *5*, 24–31. [[CrossRef](#)]
39. Johnson, N.; Sandeep, M.N. Ground Improvement Using Granular Pile Anchor Foundation. *Procedia Technol.* **2016**, *24*, 263–270. [[CrossRef](#)]
40. Muthukumar, M.; Shukla, S.K. Comparative Study on the Behaviour of Granular Pile Anchors and Helical Pile Anchors in Expansive Soils Subjected to Swelling. *Int. J. Geotech. Eng.* **2017**, *14*, 49–54. [[CrossRef](#)]

41. Muthukumar, M.; Shukla, S.K. Swelling Behaviour of Expansive Clay Beds Reinforced with Encased Granular Pile Anchors. *Int. J. Geotech. Eng.* **2016**, *12*, 109–117. [[CrossRef](#)]
42. Abbas, H.O. Laboratory Study on Reinforced Expansive Soil with Granular Pile Anchors. *Int. J. Eng.* **2020**, *33*, 1167–1172. [[CrossRef](#)]
43. Sharma, A.; Sharma, R.K. An Experimental Study on Uplift Behaviour of Granular Anchor Pile in Stabilized Expansive Soil. *Int. J. Geotech. Eng.* **2021**, *15*, 950–963. [[CrossRef](#)]
44. Khan, H.A.; Gaddam, K. An Experimental Study on Heave and Uplift Behaviour of Granular Pile Anchor Foundation System. *IOP Conf. Ser.: Earth Environ. Sci.* **2021**, *822*, 012038. [[CrossRef](#)]
45. Pack, J.S. Performance of Square Shaft Helical Pier Foundations in Swelling Soils. *Geotech. Pract. Publ.* **2007**, 76–85. [[CrossRef](#)]
46. Chao, K.C.; Nelson, J.D.; Overton, D.D. Factors Influencing Design of Deep Foundations on Expansive Soils. In Proceedings of the 5th Asia Pacific Conference on Unsaturated Soils, Pattaya, Thailand, 14–16 November 2011; Volume 2, pp. 829–834.
47. Al-Busoda, B.S.; Abbasi, H.O. Mitigation of Expansive Soil Problems by Using Helical Piles with Additives. *J. Geotech. Eng.* **2015**, *2*, 30–40.
48. Al-Busoda, B.S.; Abbasi, H.O. Helical Piles Embedded in Expansive Soil Overlaying Sandy Soil. *Al Khwarizmi Eng. J.* **2016**, *12*, 19–25.
49. Albusoda, B.S.; Abbasi, H.O. Performance Assessment of Single and Group of Helical Piles Embedded in Expansive Soil. *Int. J. Geo. Eng.* **2017**, *8*, 25. [[CrossRef](#)]
50. Mulyanda, D.; Iqbal, M.M.; Dewi, R. The Effect Of Helical Size On Uplift Pile Capacity. *Int. J. Sci. Technol. Res.* **2020**, *9*, 4140–4145.
51. Joseph, J.; Kumar, S.; Sawant, V.A.; Patel, J.B. An Experimental and Numerical Comparative Study on the Uplift Capacity of Single Granular Pile Anchor and Rough Pile in Sand. *Int. J. Geotech. Eng.* **2021**, *16*, 499–513. [[CrossRef](#)]
52. Alwalan, M.; Alnuaim, A. Axial Loading Effect on the Behavior of Large Helical Pile Groups in Sandy Soil. *Arab. J. Sci. Eng.* **2022**, *47*, 5017–5031. [[CrossRef](#)]
53. Mahmoudi-Mehrzi, M.E.; Ghanbari, A.; Sabermahani, M. The Study of Configuration Effect of Helical Anchor Group on Retaining Wall Displacement. *Geomech. Geoengin.* **2020**, *17*, 598–612. [[CrossRef](#)]
54. Lin, Y.; Xiao, J.; Le, C.; Zhang, P.; Chen, Q.; Ding, H. Bearing Characteristics of Helical Pile Foundations for Offshore Wind Turbines in Sandy Soil. *J. Mar. Sci. Eng.* **2022**, *10*, 889. [[CrossRef](#)]
55. Chaghameh, A.; Arjomand, M.; Adresi, M. Screw Pile and Its Application in Road's Subgrade Improvement. *Road* **2022**, *30*, 197–206.
56. Joseph, J.; Kumar, S.; Patel, J.B.; Sawant, V.; Tandel, Y. Model Tests on Granular Pile Anchor and Helical Anchor: A Comparative Study. *Int. J. Geosynth. Ground Eng.* **2022**, *8*, 44. [[CrossRef](#)]
57. Sabatini, P.J.; Pass, D.G.; Bachus, R.C.; Consultants, G. *Ground Anchors and Anchored Systems*; Office of Bridge Technology, Federal Highway Administration: Washington, DC, USA, 1999.
58. Al-Busoda, B.S.; Awn, S.H.A.; Abbasi, H.O. Numerical Modeling of Retaining Wall Resting on Expansive Soil. *Geotech. Eng. J. SEAGS AGSSEA* **2017**, *48*, 116–121.
59. Al-Busoda, B.S.; Abbas, H.O. Numerical Simulation of Mitigation of Soil Swelling Problem under Communication Tower Using Helical Piles. *J. Geotech. Eng.* **2017**, *4*, 35–46.
60. Alsirawan, R.; Alnmr, A. Dynamic Behavior of Gravity Segmental Retaining Walls. *Pollack Period.* **2022**, *18*, 94–99. [[CrossRef](#)]
61. Law, K.H.; Geotechnical, K.H.; Bhd, S. 3D Finite Element Analysis of a Deep Excavation Considering the Effect of Anisotropic Wall Stiffness Impact. In Proceedings of the 19th Southeast Asian Geotechnical Conference & 2nd AGSSEA Conference (19SEAGC & 2AGSSEA), Kuala Lumpur, Malaysia, 31 May–3 June 2016.
62. Al-Ani, W.; Wanatowski, D.; Chan, S.H. Numerical Analysis of Piled Embankments on Soft Soils. In Proceedings of the Geo. Shanghai, Shanghai, China, 5 May 2014; American Society of Civil Engineers (ASCE): Reston, VA, USA; pp. 30–39.
63. Hsiung, B.C.B.; Yang, K.H.; Aila, W.; Ge, L. Evaluation of the Wall Deflections of a Deep Excavation in Central Jakarta Using Three-Dimensional Modeling. *Tunn. Undergr. Space Technol.* **2018**, *72*, 84–96. [[CrossRef](#)]
64. Alnmr, A. Material Models to Study the Effect of Fines in Sandy Soils Based on Experimental and Numerical Results. *Acta Tech. Jaurinensis* **2021**, *14*, 651–680. [[CrossRef](#)]
65. Liu, Y.; Vanapalli, S.K. Mechanical Behavior of a Floating Model Pile in Unsaturated Expansive Soil Associated with Water Infiltration: Laboratory Investigations and Numerical Simulations. *Soils Found.* **2021**, *61*, 929–943. [[CrossRef](#)]
66. Nowkandeh, M.J.; Choobbasti, A.J. Numerical Study of Single Helical Piles and Helical Pile Groups under Compressive Loading in Cohesive and Cohesionless Soils. *Bull. Eng. Geol. Environ.* **2021**, *80*, 4001–4023. [[CrossRef](#)]
67. Elsherbiny, Z.H.; El Naggar, M.H. Axial Compressive Capacity of Helical Piles from Field Tests and Numerical Study. *Can. Geotech. J.* **2013**, *50*, 1191–1203. [[CrossRef](#)]
68. Han, Z.; Vanapalli, S.K.; Kutlu, Z.N. Modeling Behavior of Friction Pile in Compacted Glacial Till. *Int. J. Geomech.* **2016**, *16*, D4016009. [[CrossRef](#)]
69. Alnmr, A.; Ray, R.P.; Alsirawan, R.; Yang, H.-W.; Wang, S.; Cao, C.; Alnmr, A.; Ray, R.P.; Alsirawan, R. A State-of-the-Art Review and Numerical Study of Reinforced Expansive Soil with Granular Anchor Piles and Helical Piles. *Sustainability* **2023**, *15*, 2802. [[CrossRef](#)]

70. Kaufmann, K.L.; Nielsen, B.N.; Augustesen, A.H. Finite Element Investigations on the Interaction between a Pile and Swelling Clay. 2010. Available online: <https://vbn.aau.dk/en/publications/finite-element-investigations-on-the-interaction-between-a-pile-a> (accessed on 23 June 2023).
71. Tripathy, S.; Subba Rao, K.S.; Fredlund, D.G. Water Content—Void Ratio Swell-Shrink Paths of Compacted Expansive Soils. *Can. Geotech. J.* **2011**, *39*, 938–959. [[CrossRef](#)]
72. Estabragh, A.R.; Parsaei, B.; Javadi, A.A. Laboratory Investigation of the Effect of Cyclic Wetting and Drying on the Behaviour of an Expansive Soil. *Soils Found.* **2015**, *55*, 304–314. [[CrossRef](#)]
73. Al-Shamrani, M.A.; Dhowian, A.W. Experimental Study of Lateral Restraint Effects on the Potential Heave of Expansive Soils. *Eng. Geol.* **2003**, *69*, 63–81. [[CrossRef](#)]
74. Thakur, V.; Narain Singh, D.; Thakur, V.K.S.; Singh, D.N. Rapid Determination of Swelling Pressure of Clay Minerals. *J. Test. Eval.* **2005**, *33*, 239–245. [[CrossRef](#)]

Disclaimer/Publisher’s Note: The statements, opinions and data contained in all publications are solely those of the individual author(s) and contributor(s) and not of MDPI and/or the editor(s). MDPI and/or the editor(s) disclaim responsibility for any injury to people or property resulting from any ideas, methods, instructions or products referred to in the content.